UNIVERSIDADE FEDERAL DO RIO DE JANEIRO

INSTITUTO DE FÍSICA

DETECTING ENTANGLEMENT THROUGH MEASUREMENTS OF CHARACTERISTIC FUNCTION OF TWO PHOTONS

Khalilullah Khan

Dissertação de Mestrado apresentada ao Programa de Pós-Graduação em Física do Instituto de Física da Universidade Federal do Rio de Janeiro - UFRJ, como parte dos requisitos necessários à obtenção do título de Doutor em Ciências (Física).

Orientador: Gabriel Horacio Aguilar

Rio de Janeiro

Março de 2020

αxxx Khalilullah Khan

DETECTING ENTANGLEMENT THROUGH MEASUREMENTS OF CHARACTERISTIC FUNCTION OF TWO PHOTONS/Khalilullah Khan - Rio de Janeiro: UFRJ/IF, 2020.

xiv, 154f.

Orientador: Gabriel Horacio Aguilar

Dissertação (mestrado) - UFRJ / Instituto de Física / Programa de Pós-graduação em Física, 2020.

Referências Bibliográficas: f. 124-145.

1. Introduction. 2. Preliminaries. 3. Entanglement criteria. 4. Experiment. 5.Conclusion. I. Gabriel Horacio Aguilar . II. Universidade Federal do Rio de Janeiro, Instituto de Física, Programa de Pós-graduação em Física. III. Detecting entanglement through measurements of characteristic function of two photons.

Resumo

DETECTING ENTANGLEMENT THROUGH MEASUREMENTS OF CHARACTERISTIC FUNCTION OF TWO PHOTONS

Khalilullah Khan

Orientador: Gabriel Horacio Aguilar

Resumo da Dissertação de Mestrado apresentada ao Programa de Pós-Graduação em Física do Instituto de Física da Universidade Federal do Rio de Janeiro - UFRJ, como parte dos requisitos necessários à obtenção do título de Mestre em Ciências (Física).

Nesta tese, usamos o processo de conversão descendente paramétrica espontânea (CPDE) em uma nova geometria de dois cristais e geramos pares de fótons emaranhados em polarização. Os efeitos espaciais observados em pares de fótons gerados por espalhamento paramétrico fornecem um campo de teste poderoso e fértil para protocolos de informação quântica e para explorar conceitos fundamentais da mecânica quântica. Muita atenção tem sido dada à medição das funções características de posição e das distribuições de probabilidade de momento. Curiosamente, estabelecemos uma nova relação de incerteza a partir das funções características de variáveis espaciais transversais de um par de fótons. Essas novas relações de incertezas forneceram um novo método para verificar uma correlação não-local não-trivial em um estado de dois fótons gêmeos gerados pelo processo de conversão paramétrica espontânea. Até o momento, nenhum critério de emaranhamento perfeito para estados de variáveis contínuas não-Gaussiano foi explorado. Portanto, a criação de critérios de emaranhamento em estados não-Gaussianos é, de fato, essencial

para estudar esse fenômeno surpreendente de maneira eficiente.

Palavras-chave: Conversão descendente paramétrica espontânea, Função característica, relação de incerteza, Emaranhamento Gaussiano, Emaranhamento não-Gaussiano.

Abstract

DETECTING ENTANGLEMENT THROUGH MEASUREMENTS OF CHARACTERISTIC FUNCTION OF TWO PHOTONS

Khalilullah Khan

Orientador: Gabriel Horacio Aguilar

Abstract da Dissertação de Mestrado apresentada ao Programa de Pós-Graduação em Física do Instituto de Física da Universidade Federal do Rio de Janeiro - UFRJ, como parte dos requisitos necessários à obtenção do título de Mestre em Ciências (Física).

In this thesis, we used the process of Spontaneous parametric down-conversion in a novel two-crystal geometry and generated polarization-entangled photon pairs. The observed spatial effects in photon pairs generated by parametric scattering provide a powerful and fertile testing ground for quantum information protocols and for exploring fundamental concepts of quantum mechanics. Much attention has been paid to the measurement of the characteristic functions of quantum mechanical position and momentum probability distributions. Interestingly, we have established a new relationship of uncertainty from the characteristic functions of transverse spatial variables of a pair of photons. These new relations of uncertainties provided a new method for verification of a non-trivial non-local correlation in a state of two twin photons generated by the process of spontaneous parametric down-conversion. Up to now, no perfect entanglement criterion for the non-Gaussian continuous variable state is explored. Hence, the invention of entanglement criteria in non-Gaussian states is, in fact, essential to study this amazing phenomenon

efficiently.

Keywords: Spontaneous parametric down-conversion, Characteristic function, uncertainty relation, Gaussian Entanglement, Non-Gaussian Entanglement.

Acknowledgments

All praises and glory belong to Allah, The Almighty, The most Merciful and beneficent, Who give me the potential to complete my research within the given period of time successfully. I also want to pay my gratitude to the Holy Prophet (SAW) P.B.U.H who is the perfect source of knowledge and guidance for all the humanity.

I am indebted to so many people for their help, without which I could not complete my research. My first and greatest thanks go to Dr. Gabriel Horacio Aguilar for being the perfect thesis supervisor. Although, I joined the group without any knowledge about optics experiments, he was patient with my slow progress, navigated my research direction, and gave me brilliant suggestions whenever I was stuck with various obstacles. I am excited to pursue my PhD under his supervision.

I feel deeply thankful to my labmates who made my research in our group extremely pleasant: Thais, Muriel, Rodrigo and Kei. I learned a lot from them about the experiments. Also, they helped me with the optics equipments.

The past 2 years in Rio de Janeiro would not have been possible without the many friends that I have made here. Thanks go to Quaid, Rajwali Khan, Rafaqat, Rafi, Asmat, Hamza, Adnan, Tahir, Abrar, Sebastio, Mariana, Rodrigo, Victor, Saba and everyone in IF UFRJ. Also i am very thankful to my pakistani friends Noor islam and Zaiba for their unconditional support.

My warmest thanks to Denilucy Feitosa Nunes for her love, friendship and motivation throughout my studies in brazil.

I would like to thank my parents Amanullah Khan and Akhtar begum, my sisters Manahil Sunbal and Asal Musaffa, and my brother Asad Ullah, whose continuous prayers and support made this achievement possible.

Finally, I like to thank the brasilian funding agency Coordenação de Aperfeiçoamento de

Pessoal de Nível Superior (CAPES) for their financial support.

Contents

List of Figures

Chapter 1

Introduction

The quantum information (QI) field links concepts from quantum physics, information theory, and computer science to study the implications that the laws of quantum mechanics improve the way we send, process and compute informations. A quantum computer [1] uses quantum mechanical two-level systems ("qubits") instead of the classical bits to store information and apply unitary transformations to process this information. The main benefits of quantum computation comes from the superposition principle. The number of parameters describing a quantum system that can be used to encode information for the purpose of computing grows exponentially in the number of qubits, whereas in the classical system it grows linearly in the number of bits. Therefore, quantum computers are complex interferometric devices that provide a unique sort of parallelism of computational states described by these parameters.

In the meantime, quantum information research has produced many surprising insights into the properties of quantum mechanics that are of fundamental interest regardless of potential applications. Among all of the astounding properties, entanglement may be one of the most interesting, that is the existence of non-local, non-trivial correlations between the components of a composite system. This surprising property was first studied and named by Erwin Schrodinger in 1935 and was investigated in the seminal paper of Einstein, Podolsky, and Rosen, the EPR paper [2] in their attempt to point out the incompleteness of a quantum description of reality. This turned out to be the basic idea leading to

the famous Bell's inequality invented to enable experimental discrimination between the classical correlation and quantum correlation [3]. In 1982 Alain Aspect conducted an experiment following Bell's idea and verified the correctness of the quantum correlation [4].

Communication technology and information processing are greatly enhanced by employing many counter-intuitive properties of quantum systems such as superposition of states, uncertainty principle and entanglement. In 1991 Artur Ekert proposed E91 communication protocol and demonstrated that it's possible to develop a much more secure protocol than other classical methods [5]. Also, in biological and chemical systems, entanglement is considered a crucial phenomenon such as stability of DNA double helix [6]. Thus, it's very important in quantum information task to identify if the involed systems are entangled.

In this dissertation we work with continuous variable (CV) systems. A CV system represents system whose Hilbert space is infinte dimensional and is different from discrete variable (DV) system such as spin of particle whose Hilbert space is finite. In particular a bipartite (two-particle or two-mode system) continuous variable (CV) entangled state is the state that can't be expressed in terms of a summation of tensor products between two subsystems density matrices as described in entanglement section. Properties and behavior of these subsystems are correlated in a non-trivial form.

The usual context in which CV are studied is the Gaussian states. The Gaussian states are characterized by a Gaussian Wigner function. In our work we will study criteria of entanglement for non-Gaussian states. Non-Gaussian states are characterized by a non-Gaussian Wigner function. Entanglement in these states is important to explore because it yields promising results that lead to the improvement of different communication protocols [7, 8]. Samuel and Peter declared that the true power of quantum mechanics can only be exploited through non-Gaussian states and non-Gaussian interactions [9]. In quantum optics the photon number states (Fock states) are an example of a non-Gaussian states.

The invention of entanglement criteria and measures are essential to describe entanglement efficiently. In 2016 Rudnicki et al. [10] developed a new relation of uncertainty from characteristic function and used this relation to establish new entanglement criteria in non-Gaussian states obtained from measurements on the polarization of photons. However, till now no perfect entanglement criterion and measure for non-Gaussian CV state exist. Thus, it's necessary to establish a better criterion and measure for this particular system.

The main purpose of this dissertation is to identify entanglement in non-Gaussian states through the measurement of the characteristic function of two photons. In chapter 2 we introduced some quantum phenomena like Entanglement, Gaussian entanglement, non-Gaussian entanglement, Spontaneous Parametric down conversion (SPDC). Further, we explain optical phenomena such as polarization and optical elements such as Half Wave Plate (HWP), Quarter Wave Plate (QWP), Polarizing Beam Splitter (PBS). Finally, we explain the characteristic functions.

In chapter 3, we explain entanglement criteria for a discrete variable (finite-dimensional) system and explored entanglement criteria with the emphasis on the Peres-Horodecki method. This is to provide more basic backgrounds before considering continuous variable (infinite-dimensional) systems. Further we explain entanglement criteria for gaussaian states and explain a necessary and sufficient condition of entanglement in gaussian states. In section 3.2 a criteria for continuous variable entanglement in non-gaussian states are explained. Finally we demonstrate an inequality that is used to identify entanglement through measurement of characteristic function.

In chapter 4 we explain briefly the experimental setup that we use to measure the characteristic function through polarization measurements. After presenting a proposal we make the calculation for pure states. However, the experimental states are not pure and we study how the mixing of the states affects the proposed scheme. Furthermore we show how to use this setup to test new relations of uncertainty. Violation of the uncertainty relation witnesses entanglement in non-gaussian states.

Finally, the conclusion will be discussed briefly in chapter 5.

Chapter 2

Preliminaries

Quantum optics is a research field that uses semi-classical and quantum mechanical physics to investigate phenomenon involving light and its interaction with matter at microscopic level. During the past decade, important new developments in optics took place due to the availability of new light sources such as the laser. Also, improvement in detection techniques, allowing one to detect very weak and fast signals, played an important role in the development of quantum optics.

2.1 Quantum Entanglement

We will start with the definition of entanglement for the simplest case; the pure states. Here it will be clear why the entanglement originates from the superposition principle.

We consider a system S composed of N particles. Let's call this kind of system a multipartite system (for N=2 the system will be bipartite). We use the quantum description, where the total space of state is a Hilbert space H, resulting from the tensor product of the individual N Hilbert spaces of each subsystem: $H = H_1 \otimes H_2 \otimes ...H_N$, where H_i with $1 \leq i \leq N$ are Hilbert space of dimension d_i correspond to the subsystem i. The dimension of total space H is $D = \Pi_i^N d_i$. The structure of H is such that it's not necessarily that all of its elements are the product of others two elements. If we consider $|j_i\rangle$ with $0 \leq j_l \leq d_l - 1$ to the element of a convenient basis of H_l, the principle of superposition

allows to write the most general pure state of the multipartite system as

$$|\Phi\rangle = \sum_{j_1,\ldots,j_N} \Phi_{j_1} |j_1\rangle \otimes \ldots \otimes |j_N\rangle. \tag{2.1}$$

We can see that this state cannot be written in general as a product state of the individual states of the subsystems given by

$$|\Phi\rangle = |\Phi_1\rangle \otimes \ldots \otimes |\Phi_n\rangle. \tag{2.2}$$

In other words, we see that in general it is not possible to designate a single state vector for each individual system, and the systems can be found in different states, each of these states with a certain probability. From here the definition of entanglement comes.

A pure state is entangled if and only if, we cannot write it as a product state. A typical example for bipartite systems, i.e for N=2, with the dimension of each subsystem $d_1 = d_2 = 2$ are the famous Bell states

$$|\Phi^{\pm}\rangle = \frac{1}{\sqrt{2}}\big(|0\rangle_A \otimes |0\rangle_B \pm |1\rangle_A \otimes |1\rangle_B\big), \tag{2.3}$$

$$|\Psi^{\pm}\rangle = \frac{1}{\sqrt{2}}\big(|0\rangle_A \otimes |1\rangle_B \pm |1\rangle_A \otimes |0\rangle_B\big), \tag{2.4}$$

where $|j\rangle_i$ represents the system i in state j. These four states constitute an orthonormal basis of maximally entangled states for the space of two qubits and can therefore be distinguished by suitable measurements. The Bell states have the following notable property: the individual state of the qubits, regardless of what happens to each other, is a state completely mixed. To see this mathematically, we must apply a trace over the qubit that is being ignored, obtaining

$$\rho_B = Tr_A\big(|\Phi^+\rangle\langle\Phi^+|\big) = \sum_{i=0,1} {}_1\langle i|\Phi^+\rangle\langle\Phi^+|i\rangle_1 = \frac{1}{2}|0\rangle_2\langle 0| + |1\rangle_2\langle 1| = \frac{1}{2}\mathbb{I}. \tag{2.5}$$

We see that the reduced density matrix is proportional to the identity, so all the results measurements are equally probable. Therefore, looking at just one of the subsytems, we are not aware of the global structure; only a measurement can reveal the information of this structure.

2.2 Spontaneous parametric down-conversion

The entanglement that we will study in this thesis was obtained experimentally through Spontaneous parametric down-conversion (SPDC). SPDC was firstly described theoretically by D. Klyshko and his fellows and experimentally observed by D. C. Burnham and D. L. Weinberg in 1970 [11, 12, 13]. Carroll Alley and Yanhua Shih, Rupamanjari Ghosh and Leonard Mandel applied SPDC to experiments in 1980 [14]. Nowadays, SPDC plays a very important role in quantum optics experiments for applications in quantum computation [15], quantum metrology [16] and quantum cryptography [17]. It can also be used for testing basic laws of quantum mechanics [18].

In SPDC, a nonlinear birefringent crystal is typically pumped by an intense pump laser beam, producing low intensity signal and idler fields. The pump laser has frequency ω_p and is typically in the UV or violet region, while the down-converted signal and idler fields have frequencies ω_s and ω_i that are usually in the visible or near infra-red region of the spectrum. The wave vector of pump, signal and idler field is denoted by $\mathbf{k}_p$, $\mathbf{k}_s$ and $\mathbf{k}_i$ respectively. Due to various constraints and conservation laws, the quantum state of down converted photons is non-separable, in other words we cannot write the quantum state as a product of two one-photon states.

SPDC respects the law of conservation of energy and momentum, such that the combined energy and momentum of a pair of entangled photons will be equal to pump photon

$$\hbar\omega_p = \hbar\omega_s + \hbar\omega_i, \tag{2.6}$$

$$\mathbf{k}_p = \mathbf{k}_i + \mathbf{k}_s \quad and \quad \Delta\mathbf{k} = \mathbf{k}_p - \mathbf{k}_i - \mathbf{k}_s = \mathbf{0}. \tag{2.7}$$

Equation (2.7) is phase matching condition. The conditions imposed by equations (2.6) and (2.7) are pictorially represented in figure 2.1.

Birefringent materials are normally used for phase-matching conditions. There are two ways of satisfying the phase matching conditions in uni-axial birefringent crystal known as type-I and type-II. In type-I phase matching the signal and idler photon contributes same

polarization (ordinarily) while the pump photon polarized perpendicular to ordinarily direction, *i.e* pump photon polarized in extraordinary direction. The highest conversion efficiency of SPDC obtained so far is of the order of 4 pairs per 10^6 incoming photons for PPLN in waveguides, which is typically very low [19].

Depending on the phase matching, the output of the down-converted light is emitted in the form of cones. For the case of the type-I the down-converted light is emitted in the form of a single cone. Pair of photons are emitted on the opposite side of the cone sharing the same polarization. One of the most used crystals for this type-I conversion are BBO (beta-Barium Borate) crystals.

Up to now physicist used SPDC to generate photons which are entangled in polarization [20, 21] , energy [22], linear momentum [23], and orbital angular momentum [24, 25], among other degrees of freedom.

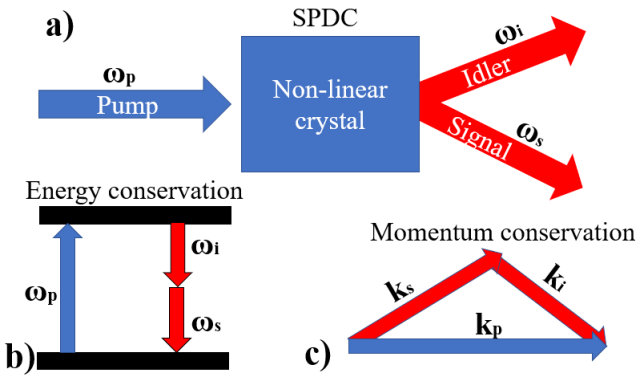

Fig. 2.1: a)SPDC, photon of energy $\hbar w_p$ splits into two photons with energies $\hbar w_i$ and $\hbar w_s$ respectively, b) and c) is representation of energy and momentum conservation of SPDC .

2.3 Spatial Variables

Many experiments performed in the 1990s strongly suggested that photon pairs produced by SPDC were indeed entangled in transverse spatial degrees of freedom [26]. In 2004, Howell et al. and D'Angelo et al. demonstrated that the pairs of down-converted photons are indeed entangled by experimentally violating separability criteria [27, 28]. These

experiments utilize criteria of entanglement involving measurements of difference and sum of position and momentum variables. These global operators for the spatial degrees of photon pairs can be written as

$$\mathbf{X}_{\pm} = \mathbf{x}_1 \pm \mathbf{x}_2, \tag{2.8}$$

$$\mathbf{P}_{\pm} = \mathbf{p}_1 \pm \mathbf{p}_2, \tag{2.9}$$

where $\mathbf{x}_i$ with $i = 1, 2$, is position of the i photon and $\mathbf{p}_i$ represents the momentum of i photon. Also we assume that $[\mathbf{x}_j, \mathbf{p}_k] = i\delta_{j,k}$ and $j, k = 1, 2$. In case of transverse spatially entangled photons, the position and momentum observables correspond to measurements in the near and in the far-field respectively, relative to the source plane, namely the SPDC crystal. The far field is associated with a momentum measurement at the source plane while the near field is associated with a position measurement at the source plane.

2.3.1 Gaussian Entanglement

A Gaussian state is the simplified but non-trivial group of continuous variable systems. The Wigner function of Gaussian state is a Gaussian function. Therefore, information about variance and mean will be sufficient to describe a state. These are states of minimum uncertainty that precisely characterize many optical system like LASER (coherent states) and thermal states. Therefore, Gaussian states are interesting and important because of its simple mathematics and broad applications in many optical systems. Thermal, coherent and squeezed states are types of Gaussian states. Entanglement in Gaussian states is identified through violation of one of a number of inequalities, which serve as entanglement witnesses. For example, Mancini-Giovannetti-Vitali-Tombesi (MGVT) criteria is [29]

$$\langle \Delta^2 \mathbf{X}_{\pm} \rangle \langle \Delta^2 \mathbf{P}_{\mp} \rangle \geq 1, \tag{2.10}$$

where Δ^2 in equation (2.10) stands for variance. Also the separability principle of Duan, Giedke, Cirac and Zoller (DGCZ) reads [30]

$$a^2\langle\Delta^2\mathbf{X}_{\pm}\rangle + \frac{1}{a^2}\langle\Delta^2\mathbf{P}_{\mp}\rangle \geq 2, \tag{2.11}$$

where a is local scaling parameter which makes the quantities in the sum dimensionless. All separable states will obey equations (2.10) and (2.11). Violation of any of the above inequalities will be a sufficient condition to identify quantum entanglement.

A necessary and sufficient condition for $1 \times N$ mode gaussian states were proposed by Simon [31] which is basically a generalization of the Peres-Horodecki criterion to CV systems. We will explain entanglement criteria in more detail in third chapter. To evaluate this, its mandatory to reconstruct the covariance matrix [32]. Violation of Simon, MGVT or DGCZ criteria are sufficient for identifying the quantum states with negative partial transpose (NPT). Generally for Gaussian states, these criteria are not necessary condition for entanglement due to the existence of bound entangled states which have a positive partial transpose.

2.3.2 Non-Gaussian Entanglement

An example of non-Gaussian state is the photon number state, Fock state in quantum optics. For this kind of states the first and second statistical moments are not sufficient to describe it. Furthermore, these states are harder to deal experimentally because it requires other techniques than the Gaussian operations which are more complicated or sensitive to conditions, such as photon counting. However, there are ideas which used non-Gaussian states to enhance efficiency of quantum technology. For instance, non-Gaussian states can improve the efficiency and robustness of a continuous variable quantum teleportation protocol significantly compared to Gaussian states [32]. Furthermore entanglement in non-Gaussian states yields promising results that lead to the improvement of different communication protocols [7, 8]. Samuel and Peter declared that the true power of

quantum mechanics can only be exploited through non-Gaussian states and non-Gaussian interactions [9]. Therefore, non-Gaussian systems are also interesting and important, despite of its complication.

In case of non-Gaussian states, these second order criteria are not necessary, but are sufficient. The second order criteria are not violated because there exist NPT entangled states. We can use NPT criteria of Shchukin and Vogel in this case [33]. This shows that Simon criterion and inequalities are special cases of general NPT criteria. A sufficient condition for entanglement is to violate any inequality in Shchukin-Vogel hierarchy. The violation will indicate that the quantum state is NPT. The state is entangled when we identify the nonpositivity of partial transposition. From the Shchukin–Vogel criterion higher-order inequalities are obtained. These higher-order inequalities have been violated recently for spatially non-Gaussian two-photon state which does not violate any second-order criteria [26].

2.4 Polarization

Electromagnetic plane waves consist of time-varying electric and magnetic fields that are perpendicular to each other, and perpendicular to the wave direction of travel. In a practical communication system, the electric field vector of the plane wave travelling in z-direction can have both x and y components, which oscillate independently depending on the nature of the source that generates the electromagnetic (EM) wave. The behaviour of EM waves can be determined by the orientation of the electric field vectors and this behavior is so called the polarization of the wave. Thus, polarization of the wave determines the orientation of electric field vector that lie in the plane perpendicular to the direction of propagation. For instance a monochromatic plane wave of frequency ν and angular frequency $\omega = 2\pi\nu$ propagating in the z direction with velocity equal to c. The

electric field which lies in the x-y plane is described generally by

$$\mathbf{E}(z,t) = Re\{\mathbf{A}exp[i(kz-\omega t)], \tag{2.12}$$

$$\mathbf{A} = A_{\mathrm{x}}\hat{\mathbf{x}} + A_{\mathrm{y}}\hat{\mathbf{y}}, \tag{2.13}$$

where $\mathbf{A}$ is a vector with $A_x = A_1\exp(i\phi_1)$ and $A_y = A_2\exp(i\phi_2)$ complex components. Tracing the endpoint of the vector $\mathbf{E}$(z,t) at each position z as a function of time will describe the polarization of this wave. Polarization can be categorized as linear, circular and elliptical polarization.

2.4.1 Linear Polarization

In plane wave propagation, both the electric and magnetic fields oscillates transverse to the direction of the waves. When the oscillations are in a single direction, the wave is called linearly polarized. Considering that we can decomposed the direction of electric field that propagating in the z direction into two directions with relative phase difference ϵ between the waves. The x and y components of the electric field are expressed as

$$\mathbf{E}_x(z,t) = \hat{\mathbf{x}}\, E_0 cos(kz-\omega t), \tag{2.14}$$

$$\mathbf{E}_y(z,t) = \hat{\mathbf{y}}\, E_0 cos(kz-\omega t+\epsilon), \tag{2.15}$$

where positive ϵ in equation (2.15) implies that cosine functions in both equation will not attain the same value until a later time (ϵ/ω). As an example the superposition of two perpendicular waves yield the resultant electric field described by

$$\mathbf{E}(z,t) = \mathbf{E}_x(z,t) + \mathbf{E}_y(z,t). \tag{2.16}$$

If the relative phase difference is zero or integer multiple of 2π, the waves are said to be in phase and the electric field is written as

$$\mathbf{E} = (\hat{\mathbf{x}}E_0 + \hat{\mathbf{y}}E_0)cos(kz-\omega t). \tag{2.17}$$

Equation (2.17) is the resultant wave with fixed amplitude equal to ($\hat{\mathbf{x}}E_0+\hat{\mathbf{y}}E_0$). Consider that ϵ is an odd integer multiple of $\pm\pi$ so the two orthogonal electric fields are 180° out of phase and the resultant wave is linearly polarized in the 2nd and 4th quadrants as shown in figure 2.2

$$\mathbf{E} = (\hat{\mathbf{x}}E_0 - \hat{\mathbf{y}}E_0)cos(kz - \omega t). \tag{2.18}$$

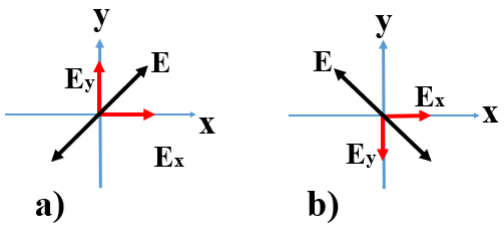

Fig. 2.2: a)E-field linearly polarized in the first and third quadrents b)E-field linearly polarized in the second and fourth quadrents.

2.4.2 Circular Polarization

Considering the two orthogonal electric fields which have equal amplitudes and relative phase difference ϵ = -π/2 +2mπ, where $m = 0, \pm1, \pm2, \ldots$. The x and y components of the electric field are

$$\mathbf{E}_x(z,t) = \hat{\mathbf{x}}\, E_0 cos(kz - \omega t), \tag{2.19}$$

$$\mathbf{E}_y(z,t) = \hat{\mathbf{y}}\, E_0 sin(kz - \omega t). \tag{2.20}$$

The resultant electric field is equal to

$$\mathbf{E} = E_0[\hat{\mathbf{x}}cos(kz - \omega t) + \hat{\mathbf{y}}sin(kz - \omega t)]. \tag{2.21}$$

The amplitude of $\mathbf{E}$ in equation (2.21) is constant but its direction is time varying and is not restricted to a single plane. At some arbitrary point z_0 and at $t = 0$ the x and y components of electric field are written as

$$\mathbf{E}_x = \hat{\mathbf{x}}\, E_0 cos(kz_0), \tag{2.22}$$

$$\mathbf{E}_y = \hat{\mathbf{y}}\, E_0 sin(kz_0). \tag{2.23}$$

At time $t = kz_0/\omega$, $\mathbf{E}_x = \hat{\mathbf{x}}E_0$, $\mathbf{E}_y = 0$, and E is along the x-axis. At this case the resultant **E** is rotating clockwise at an angular frequency ω, as seen by observer towards whom the wave is coming. Such wave is right-circularly polarized. On other hand, if the relative phase differnece is $\epsilon = \pi/2 + 2m\pi$, where $(m = 0, \pm1, \pm2, \pm3, ...)$, then the resultant **E** is be equal to

$$\mathbf{E} = E_0[\hat{\mathbf{x}}cos(kz - \omega t) - \hat{\mathbf{y}}sin(kz - \omega t)]. \tag{2.24}$$

The amplitude of **E** remains same but it rotates now counter-clock-wise and the wave is said to be left circularly polarized. Right and left hand circular polarization are shown in the figure 2.3.

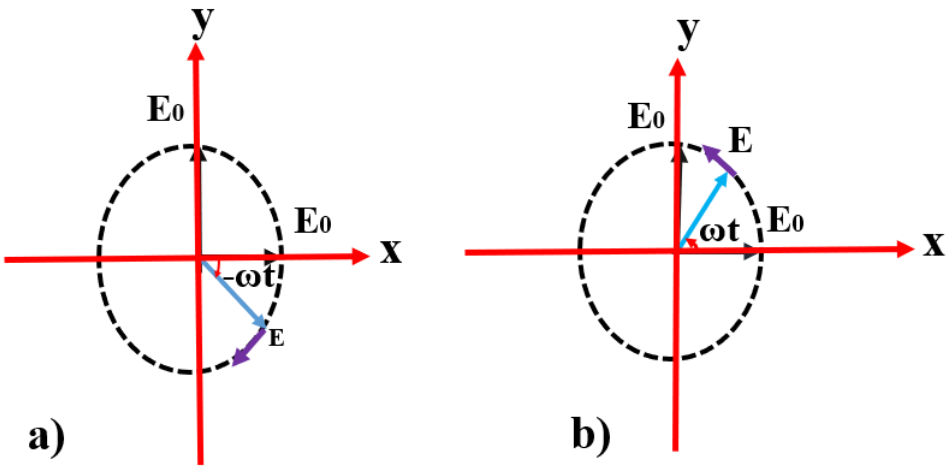

Fig. 2.3: a)Right hand circular polarization, b)Left hand circular polarization.

Adding equations (2.21) and (2.24) we get the resultant **E**-field as

$$\mathbf{E} = 2E_0\hat{x}cos(kz - \omega t). \tag{2.25}$$

This means that a linearly polarized wave can be obtained by two oppositely polarized circular waves of equal amplitude while a circularly polarized wave can be obtained by two orthogonally linearly polarized waves of equal amplitude.

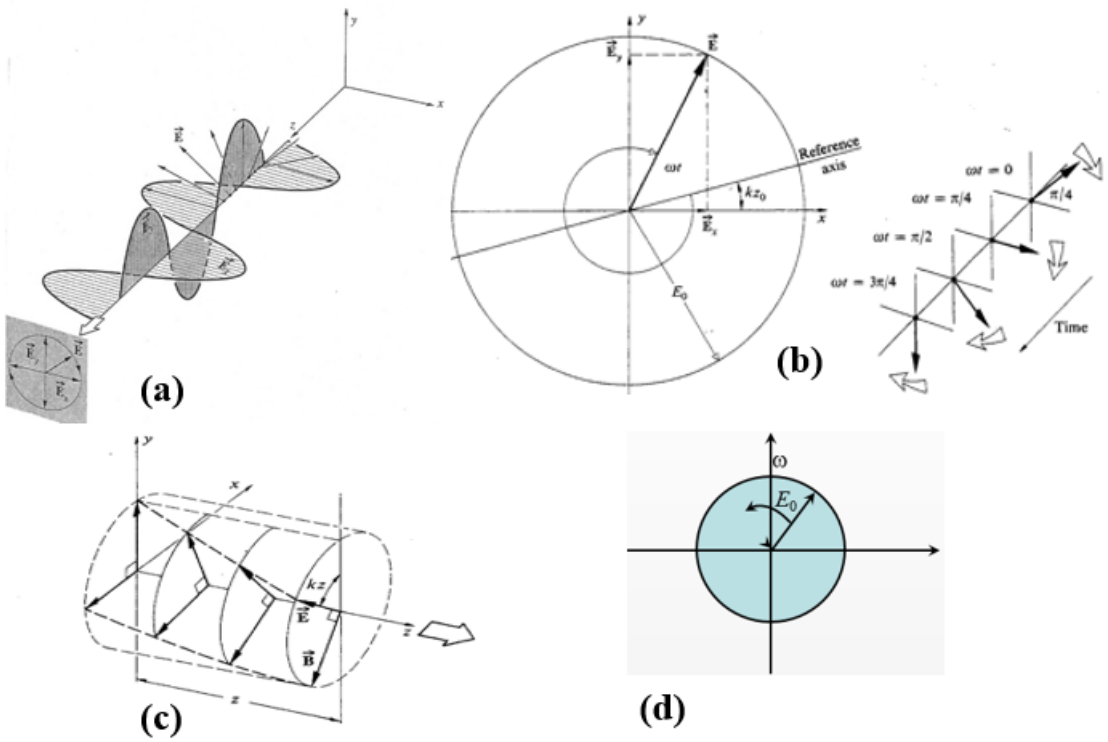

Fig. 2.4: a) Right circularly polarized wave, b) Rotation of **E** in right circular wave with rotation rate equal to ω and $kz = \pi/4$, c) Right circular polarization ($\mathscr{R}$-state) and d) Left circular poalrization ($\mathscr{L}$-state) .

2.4.3 Elliptical Polarization

It can be seen that the linear and circular polarizations are special cases of elliptical polarization. For elliptical polarization the electric field vector rotate and change its magnitude. The end point of the **E** will trace out an ellipse. A harmonic wave propagating in the z direction, its two components on the x and y axes are

$$E_x = E_{0x} cos(kz - \omega t), \tag{2.26}$$

$$\implies sin(kz - \omega t) = [1 - (E_x/E_{0x})^2]^{1/2}, \tag{2.27}$$

$$E_y = E_{0y} cos(kz - \omega t + \epsilon). \tag{2.28}$$

The searched curve equation should be independent of position and time, so we should remove $kz - \omega t$ and find the relation between E_x and E_y

$$E_y/E_{0y} = cos(kz - \omega t)cos\epsilon - sin(kz - \omega t)sin\epsilon, \tag{2.29}$$

$$E_x/E_{0x} = cos(kz - wt), \tag{2.30}$$

$$\frac{E_y}{E_{0y}} - \frac{E_x}{E_{0x}}cos\epsilon = -sin(kz - wt)sin\epsilon, \tag{2.31}$$

$$(\frac{E_y}{E_{0y}} - \frac{E_x}{E_{0x}}cos\epsilon)^2 = [1 - (E_x/E_{0x})^2]sin^2\epsilon, \tag{2.32}$$

$$(\frac{E_y}{E_{0y}})^2 + (\frac{E_x}{E_{0x}})^2 - 2\frac{E_x}{E_{0x}}\frac{E_y}{E_{0y}}cos\epsilon = sin^2\epsilon. \tag{2.33}$$

This is the equation of an ellipse in the (E_x, E_y) plane. The tilting angle α of the ellipse as shown in the figure 2.5 is given by

$$tan\ 2\alpha = \frac{2E_{0x}E_{0y}cos\epsilon}{E_{0x}^2 - E_{0y}^2}. \tag{2.34}$$

Suppose the principal axes of ellipse are aligned with the coordinate axes, that is $\alpha = 0$ or equivalently when the relative phase $\epsilon = \pm\pi/2, \pm 3\pi/2, \pm 5\pi/2, \pm 7\pi/2...$, the equation (2.33) equals to

$$(\frac{E_y}{E_{0y}})^2 + (\frac{E_x}{E_{0x}})^2 = 1. \tag{2.35}$$

By assuming $E_{0y} = E_{0x} = E_0$, equation (2.35) further reduce to equation of circle, that is $E_y^2 + E_x^2 = E_0^2$. Furthermore, if $\epsilon = 0$ or $\pm\pi$, equation (2.33) is written as

$$E_y = \pm\frac{E_{0y}}{E_{0x}}E_x. \tag{2.36}$$

These are both straight lines equations having slope $\pm\dfrac{E_{0y}}{E_{0x}}$; in other words we have linear polarization.

We can refer a particular lightwave in terms of its specific state of polarization. Right or left circularly polarized light wave is in $\mathscr{R}$- or $\mathscr{L}$- state respectively. Linearly polarized or plane-polarized light is in a $\mathscr{P}$-state which can be represented as superposition of $\mathscr{R}$- and $\mathscr{L}$-states with same amplitude, i.e $\mathscr{P} = \mathscr{R} \pm \mathscr{L}$ and elliptically polarized light wave

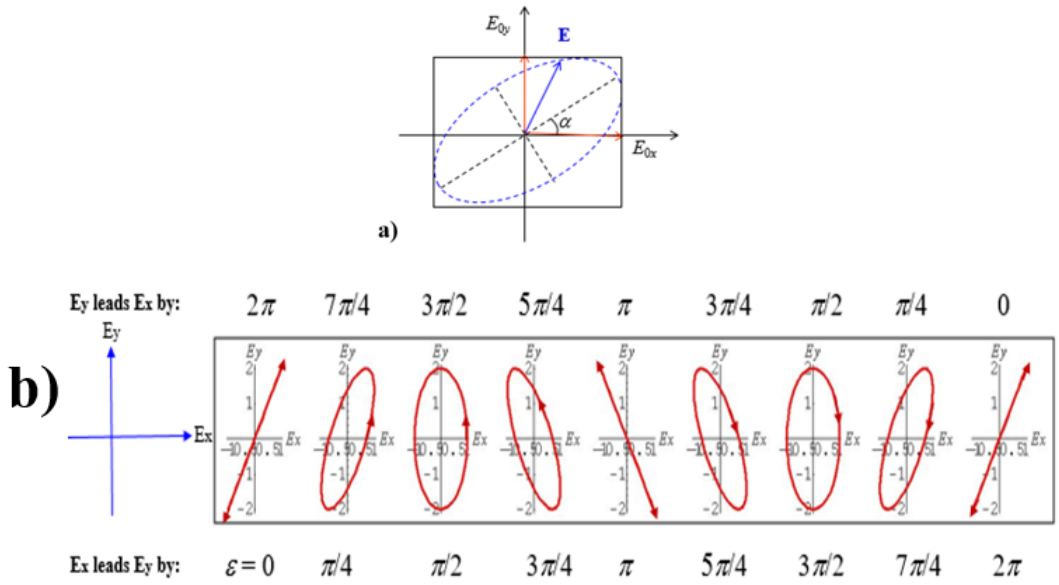

Fig. 2.5: a) Elliptical polarization, b) Different polarization configurations. Polarization would be circular with $\epsilon = \pi/2$ or $3\pi/2$.

corresponds to an $\mathscr{E}$-state which is a superposition of $\mathscr{R}$ and $\mathscr{L}$-states with different amplitudes , i.e $\mathscr{E} = a\mathscr{R} \pm b\mathscr{L}$.

2.5 Wave Plates

Retarders or waveplates (WP) are optical elements that alter the polarization of an incident light. In principle, WP operation is quite simple. One of the two constitutent coherent $\mathscr{P}$-states is somehow caused by a delay in-phase with respect to the other by predetermined amount. Upon emerging the light wave from the waveplate, there is a difference between the relative phase of the two components with respect to what it was initially, so we get a different polarization state.

A typical waveplate is a birefringet crystal normally made of mica, quartz or organic polymeric plastic, which is cut into a plate, with a proper orientation and thickness. The orientation of the cut is chosen such that the optic axis is arranged parallel to the surface of the plate. This yields two axes in the plane of the cut. The axis that is perpendicular to the optical axis is called ordinary axis, while axis that is parallel to the optical axis

is called extraordinary axis. In addition, the axis in which the light propagates faster is called fast axis. For positive uniaxial birefringent crystals ($n_e > n_o$) the axis that is perpendicular to the optic axis is the fast axis, while for negative uniaxial birefringent crystals ($n_e < n_o$) optic axis coincide with the fast axis.

An incident monochromatic plane wave has components parallel and perpendicular to the optic axis, two separate plane waves will propagate through the crystal. Since $v_{\parallel} > v_{\perp}(n_o > n_e)$ the e- wave will travel across the material faster than the o- wave. After traversing a plate of thickness d the resultant electromagnetic wave is the superposition of the e- and o-waves, which now have a relative phase difference of $\Delta\varphi$. The relative optical path-length difference is given by

$$\Lambda = d(|n_0 - n_e|). \tag{2.37}$$

Since $\Delta\varphi = k_0\Lambda$,

$$\Delta\varphi = \frac{2\pi}{\lambda_0} d(|n_0 - n_e|), \tag{2.38}$$

where λ_0 is the wavelength in vacuum. The state of the polarization of the emergent light depends on the amplitude of the incident field components and on $\Delta\varphi$.

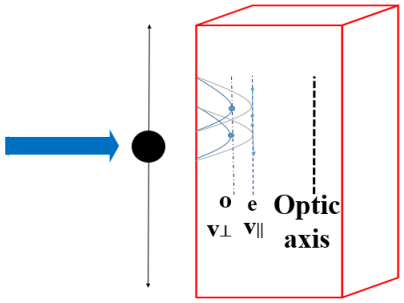

Fig. 2.6: A calcite plate cut parallel to the optic axis

2.5.1 Half-Wave Plate

Waveplate introducing a relative phase difference of π radians or 180° between the o- and e-waves is known as half-wave plate (HWP). In negative birefringent crystals the

e-wave will have a higher speed than o-wave. Considering an incident linear polarized light makes an angle θ with respect to the fast axis, the emerging wave have a relative phase shift of $\lambda_0/2$ (that is $2\pi/2$ radians), resulting an $\mathbf{E}$ rotated 2θ with respect to the field at the input of the WP. Simply for linear polarized input the HWP will rotate light initially polarized at angle θ by an angle of 2θ , as it shown in figure 2.7. Furthermore, for elliptical polarized input, HWP will flip the tilting angle and invert the handedness of circular or elliptical light, changing right to left and vice-versa as illustrated in figure 2.7.

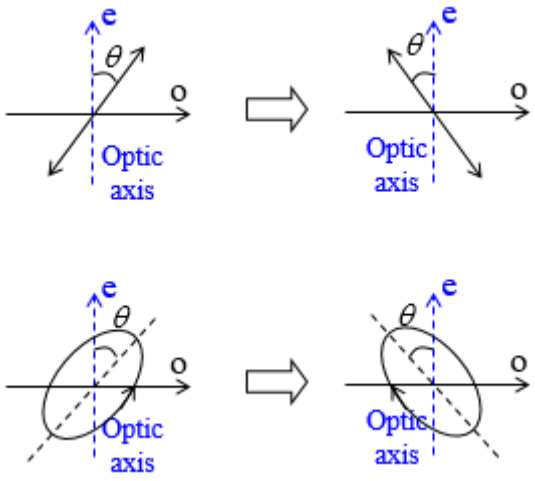

Fig. 2.7: Both can be thought as a mirror effect with respect to the fast or the slow axis.

As the e- and o- waves progress through any retardation plate, their relative phase difference $\Delta\varphi$ increases, and the state of polarization of the wave therefore gradually changes from one point in the plate to the next. If the thickness d of the material is such that it satisfy the following relation

$$d(|n_0 - n_e|) = (2m + 1)\lambda_0/2, \tag{2.39}$$

where $m = 0, 1, 2, ...$, the material acts as a half-wave plate ($\Delta\varphi = \pi, 3\pi, 5\pi\ etc$)

2.5.2 Quarter-Wave Plate

A quarter-wave plate (QWP) is a wave plate that introduces a relative phase difference of $\Delta\varphi = \pi/2$ or 90° between the constitutent orthogonal *o*- and *e*- components of a field. A significant application of QWP is to convert linearly polarized light into circularly polarized light and vice versa. Any incident linearly polarized light will divide into two components with different indices of refraction. When linear polarized light at 45° with respect to the optic axis is incident on a quarter-wave plate, its *o*- and *e*-waves have equal amplitudes, but the o-wave is retarded by a quarter of the wavelength. Under these special circumstances, a phase shift of 90° converts the wave into circular light as shown in figure 2.8. Similarly, an incident circularly polarized light change to linearly polarized light. If the thickness d of the material is such that

$$d(|n_0 - n_e|) = (4m + 1)\lambda_0/4, \tag{2.40}$$

it will function as quarter-wave plate.

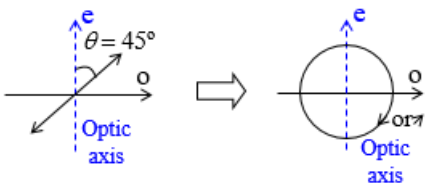

Fig. 2.8: Circularizing linearly polarization with a $\lambda/4$ waveplate.

2.5.3 Polarizing Beam Splitter

An optical device that split a beam of light depending on its polarization is called polarizing beam splitter (PBS). The PBS transmitts p-polarized light and reflects s-polarized light as shown in figure 2.9. Usually, p-polarized light has an electric field direction parallel to the plane of incidence, while s-polarized light is perpendicular to this plane. It is the crucial part for many optical experimental and measurement systems.

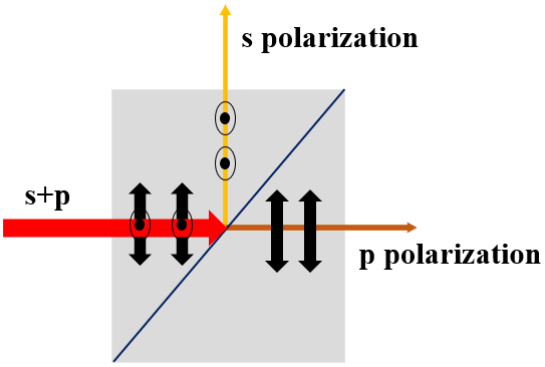

Fig. 2.9: P-polarized light is transmitted and S-polarized light reflected by 90° angle.

2.6 Production of polarization entanglement using SPDC

The polarization state of a single photon can be written as

$$|\Phi\rangle = cos(\theta/2)|H\rangle + sin(\theta/2)e^{\iota\alpha}|V\rangle, \tag{2.41}$$

where the horizontal and vertical polarization states are represented by $|H\rangle$ and $|V\rangle$, respectively. The quantum state of polarization, as the state in equation (2.41), can be used as a quantum bit (Qubit). By representing the state $|\Phi\rangle$ in the Bloch sphere, the angle θ and α are the polar and azimuthal angle, respectively. Generally, the pure state of the polarization of two photons can be written as

$$|\psi\rangle = \alpha|H\rangle_1|H\rangle_2 + \beta|H\rangle_1|V\rangle_2 + \gamma|V\rangle_1|H\rangle_2 + \delta|V\rangle_1|V\rangle_2, \tag{2.42}$$

where the amplitudes α, β, γ and δ respects the normalization condition, $|\alpha|^2 + |\beta|^2 + |\gamma|^2 + |\delta|^2 = 1$. Let's write two types of states which are entangled in polarization

$$|\phi\rangle_{1,2} = cos(\theta/2)|H\rangle_1|H\rangle_2 + sin(\theta/2)e^{i\alpha}|V\rangle_1|V\rangle_2 \tag{2.43}$$

and

$$|\psi\rangle_{1,2} = cos(\theta/2)|H\rangle_1|V\rangle_2 + sin(\theta/2)e^{i\alpha}|V\rangle_1|H\rangle_2. \tag{2.44}$$

Assuming $\theta = \pi/2$ and $\alpha = 0, \pi$ in the above equations, it can yield the complete maximally entangled states, Bell-states which were described in section (2.1).

A large number of experimental setups have been used by physicist to create polarization entangled photons. Type-I crystal source [21] and type-II crossed cone source [20] are two most common sources. For the type-I phase matching, two thin crystals in the crossed-axis configuration are used. This is the configuration we use for the experiment presented in this dissertation. The intensity of the conversion of each crystal is related with the values of $(cos(\frac{\theta}{2}))^2$, $(sin(\frac{\theta}{2}))^2$ in equations (2.43) and (2.44) and is controlled by the polarization of the pump beam. Each direction of polarization of the pumping beam (H or V) acts on only one of the crystal. Keeping the polarization of the pump beam at 45 degree, same conversion rates in the two crystals are observed. As the two crystals are positioned with perpendicular optical axes, we observe two ordinary photons produced in the first crystal or two extraordinary photons produced in the second crystal. To have entanglement in this case we need a laser source whose coherence length is greater than the seperation between the crystals and to have the two cones overlapped. The correlated photons obtained through this technique have the same polarization and we can write the obtained Bell-states as

$$|\phi\rangle^{\pm} = (|H_1, H_2\rangle \pm e^{i\alpha}|V_1, V_2\rangle)/\sqrt{2}. \tag{2.45}$$

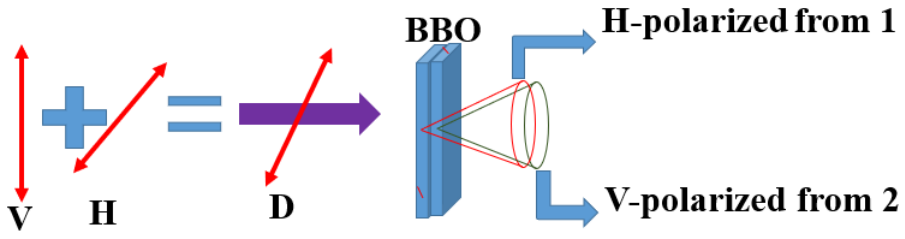

Fig. 2.10: Type-I phase matching to generate collinearly propagating photon pairs.

Another method used to generate polarized Bell states employs SPDC type-II phase

matching crystals. A type-II nonlinear crystal of thickness L creates a pair of orthogonal polarized photons, one with ordinary (vertical) polarization and the other with extraordinary (horizontal) polarization [20]. Alignment of crystal is such that that the extraordinary (e) cone and ordinary (o) cone cross at two points as shown in figure 2.11. The two detectors are placed in the direction where the cones intersect. To select the modes of interest, detectors are equipped with interference filters centered at the wavelength of interest. In our case we will use the degenerated case, where both photon have the same wavelength. The detectors are connected to an electronic system that counts the coincidences, which happens when both photons of a pair are detected. To find the maximum coincidence counts, detectors are scan in the space of transversal position. As we are searching at the intersection regime of the cone, so the photon detected in each of the detectors may have been produced with vertical or horizontal polarization. At these intersection region the quantum state detected is a Bell state

$$|\psi\rangle^{\pm} = (|H_1, V_2\rangle \pm e^{i\alpha}|V_1, H_2\rangle)/\sqrt{2}. \tag{2.46}$$

Due to the birefringence of the crystal, the down converted photons suffer transverse and longitudinal walk-off and this effect can be used to segregate between two photons. The small amount of distingusihabilty created due to walk-off degrades the quality of polarization entanglement of two photon state. This degradation can be corrected by placing a HWP after the first crystal. This plate rotates the polarization by 90°, such that when a photon passes through the second compensator crystal (width=$\frac{L}{2}$), their roles are reversed: an 'e' photon is now 'o' photon and vice versa. In this way, both photon suffer the same amount of walk-off, decreasing the spatial distinguisibilty. Another quarter and half-wave plates are placed in the path of one of the photons. Phase is adjusted by quarter wave-plate while the half wave-plate can be oriented to change the polarization of one of the photon. One can easily switch any of the four orthogonal EPR-Bell states by adjusting the angle of the wave-plates [34].

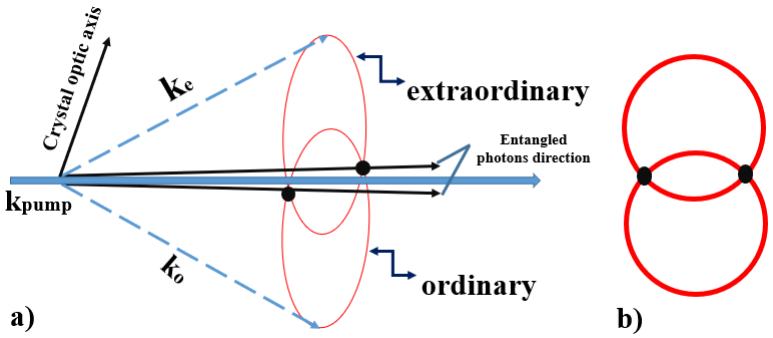

Fig. 2.11: a) SPDC cones with type-II phase matching. Correlated photons lie on opposite sides of the pump beam b) Image of down-converted photons.

2.7 Characteristic Function

The main subject of our dissertation is the characteristic function, a notation well known in classical probability theory. The characteristic function $\Phi(\lambda)$ related to a probability distribution $\rho(x)$ is defined as

$$\Phi(\lambda) = \int_{\mathbb{R}} dx\ e^{i\lambda x}\rho(x). \tag{2.47}$$

This means that, the characteristic function is the fourier transform of $\rho(x)$. For the particular case of a pure quantum state, the probability distribution is the square modulus of a wavefunction, i.e $\rho(x) = |\psi(x)|^2$. Considering this, equation (2.47) get some interesting properties. Assuming that the probability distribution in equation (2.47) is associated to the quantum mechanical position space. In this situtation the characteristic function is equal to the expected value of the momentum shift operator $e^{i\lambda\hat{x}}$, that is $\Phi(\lambda) = \langle e^{i\lambda\hat{x}}\rangle$. Second important feature of $\Phi(\lambda)$ is related to momentum representation. Consider a self-correlation function in the position representation

$$\int_{-\infty}^{\infty} \psi^*(x)\psi(x - x')dx, \tag{2.48}$$

where $\psi(x)$ is the position-space wavefunction. As the wavefunctions in position and momentum representations are connected through fourier transform given by

$$\psi(x) = \frac{1}{\sqrt{2\pi\hbar}} \int_{\mathbb{R}} dx\ e^{ipx/\hbar}\phi(p). \tag{2.49}$$

Using equation (2.49) in equation (2.48) we get

$$\tilde{\Phi}(\lambda_p) = \int_{-\infty}^{\infty} e^{-i\lambda_p p}\tilde{\rho}(p)dp = \int_{-\infty}^{\infty} \psi^*(x)\psi(x-\lambda_p)dx, \tag{2.50}$$

which is the characteristic function related to the probability distribution $\tilde{\rho}(p) = |\phi(p)|^2$, or the function of self-correlation is precisely a characteristic function. Similarly, the same holds for characteristic function defined in terms of position distribution. Consider a self-correlation function in momentum representation

$$\Phi(\lambda_x) = \int_{-\infty}^{\infty} \phi^*(p)\phi(p-p')dp, \tag{2.51}$$

where $\phi(p)$ is the state wavefunction in momentum basis. Through fourier integral

$$\phi(p) = \frac{1}{\sqrt{2\pi\hbar}} \int_{\mathbb{R}} dx\, e^{-ipx/\hbar}\psi(x). \tag{2.52}$$

By using the fourier transformation (2.52) we obtain

$$\Phi(\lambda_x) = \int_{-\infty}^{\infty} e^{i\lambda_x x}\rho(x)dx = \int_{-\infty}^{\infty} \phi^*(p)\phi(p-\lambda_x)dp, \tag{2.53}$$

which is the characteristic function related to the probability distribution $\rho(x) = |\psi(x)|^2$. Writing the characteristic functions for a two photon state $\hat{\rho}$, in term of global opertors, $\hat{x}_\pm$ and $\hat{p}_\pm$, as

$$\Phi_\pm(\lambda_x) = \langle e^{i\lambda_x \hat{x}_\pm}\rangle_{\hat{\rho}}, \tag{2.54}$$

$$\tilde{\Phi}_\pm(\lambda_p) = \langle e^{i\lambda_p \hat{p}_\pm}\rangle_{\hat{\rho}}. \tag{2.55}$$

The global operators for the spatial degrees of photon pairs are discussed in section 2:3. In case of transverse spatially entangled photons, the momentum and position observables correspond to measurements in the far and in the near-field respectively, relative to the source plane, namely the SPDC crystal.

Chapter 3

Entanglement Criteria

Quantum entanglement is a non-local and nontrivial correlation between quantum systems. It has been regarded as one of the key physical resources in quantum information tasks such as teleportation [35], quantum cryptography [36, 5], dense coding [37] and quantum computation [38]. Furthermore, in biological and chemical systems, entanglement is considered as a crucial phenomenon such as in stability of DNA double helix [6]. Therefore, it is important to find methods that can determine whether a state is entangled or not. The most simple method of witnessing entanglement consists of applying the partial trace in pure states. A state is separable if the reduced density matrix remains a pure state and in some cases if the reduced density matrix represents a mixed state then the former state is entangled. For a bipartite system

$$|\Psi\rangle_{A,B} \text{ entangled} \quad \longleftrightarrow \quad \hat{\rho}_A \text{ mixed}$$

$$|\Psi\rangle_{A,B} \text{ not entangled} \quad \longleftrightarrow \quad \hat{\rho}_A \text{ pure}$$

3.1 Peres-Horodecki criterion

Given that partial trace criteria can only be used for pure states, another methods that can be employed to identify entanglement, in both pure and mixed states, have been demonstrated by Peres-Horodecki [39], also called Positive Partial Transpose (PPT). This criterion was first proposed by Asher Peres as a condition that every separable state must

satisfy. Later, Horodecki studied the criterion in more details and discovered that it was not only a necessary but also sufficient condition for separable states of 2×2 and 2×3 dimensions. Thus for a bipartite qubit state (2×2 dimensions), this criterion can be exploited to confirm exactly whether a state is entangled or separable.

PPT criterion can be explained as follows. First, for every physical state, the density matrix must be positive-semidefinite, i.e. all of its eigenvalues must not be negative. Next, for a bipartite separable system, the density matrix can in general written as

$$\rho = \sum_{i=1}^{n} p_i \rho_{1i} \otimes \rho_{2i}, \tag{3.1}$$

where p_i is the probability of states ρ_1^i and ρ_2^i to be found in this ensemble. Assume that K is an arbitrary square matrix and L a transposition operator such that, $L(K) = (K)^T$. Performing a partial transposition into one of the subsystems is equivalent to operate $L \otimes I$ on the whole system as

$$\rho^{L_1} = (L \otimes I)\rho = \sum_{i=1}^{n} p_i L(\rho_{1i}) \otimes I(\rho_{2i}) = \sum_{i=1}^{n} p_i (\rho_{1i})^T (\rho_{2i}). \tag{3.2}$$

As the eigenvalues are preserved at transposition, this implies that $(\rho_{1i})^T$ is yet a density matrix that represents a physical state. This also implies that ρ^{L_1} must respect the positive-semidefinite property such that ρ^{L_1} represents a physical separable bipartite system. A necessary condition of the Peres criterion is that, a bipartite system will be separable if the partial transpose applied on physical density matrix yields again a positive-semidefinite matrix [39]. Later Horodecki showed that this criterion is a sufficient condition and demonstrates that states which do not satisfy this condition will be entangled states [31].

Considering a Werner state which is a sum of maximally entangled Bell-state and maximally mixed state

$$\mathscr{W} = p|\Psi^+\rangle\langle\Psi^+| + (1-p)\frac{I}{4} \tag{3.3}$$

This state will become pure by assigning 1 value to p and when p is different from 1 it is

a mixed state.

$$|\Psi^+\rangle = \frac{1}{\sqrt{2}}\Big(|01\rangle + |10\rangle\Big)$$

$$|\Psi^+\rangle\langle\Psi^+| = \frac{1}{2}\Big[\Big(|01\rangle\langle 01| + |01\rangle\langle 10| + |10\rangle\langle 01| + |10\rangle\langle 10|\Big)\Big] \tag{3.4}$$

Equation (3.3) can be expressed in term of matrix form as

$$\mathscr{W} = \frac{1}{4}\begin{bmatrix} 1-p & 0 & 0 & 0 \\ 0 & p+1 & 2p & 0 \\ 0 & 2p & p+1 & 0 \\ 0 & 0 & 0 & 1-p \end{bmatrix}. \tag{3.5}$$

To perform transposition on the first system we get

$$\mathscr{W}^{T_1} = \frac{1}{4}\begin{bmatrix} 1-p & 0 & 0 & 2p \\ 0 & p+1 & 0 & 0 \\ 0 & 0 & p+1 & 0 \\ 2p & 0 & 0 & 1-p \end{bmatrix}. \tag{3.6}$$

According to the Peres-Horodecki criterion, if $\mathscr{W}$ is separable, then $\mathscr{W}^{T_1}$ has only non-negative eigenvalues (since it must represent a physical state). In other words, if $\mathscr{W}^{T_1}$ has at least one negative eigenvalue, we know that $\mathscr{W}$ is entangled. The transition point of state from separable to entangled is related to the lowest possible value of p, i.e p_{crit} which can be calculated as

$$det(\mathscr{W}) = 0 \implies (3p+1)(1-p)^3 = 0, \tag{3.7}$$

$$det(\mathscr{W}^{T_1}) = 0 \implies (1-3p)(p+1)^3 = 0 \implies p_{crit} = 1/3. \tag{3.8}$$

Therefore, quantum state is entangled for $1 \geq p > p_{crit}$.

3.2 Criteria for Continuous Variable

In the case of CV systems, the most widespread necessary criterion for the separability of any two-mode state has been derived by Duan et al. [30] and Simon [31] simultaneously in 2000. This criterion is obtained from translating the PPT condition, which had been established for finite-dimensional discrete systems, to continuous-variable (infinite-dimensional) systems. The partial transposition of a state in continuous variables implies

simply a sign inversion of the momentum of one of the subsystems. More specifically, from the definition of the Wigner function, one can obtain the following equivalence

$$W^{PT}(x_1, p_1, x_2, p_2) = W(x_1, p_1, x_2, -p_2). \tag{3.9}$$

Therefore, the partial transposition can be understood as a mirror reflection in the phase space or a time reversal on mode 2, which inverts only coordinate of p_2. As stated by Simon [31], the PPT criterion can be translated in the continuous-variable framework as follows: if ρ is separable, then its Wigner distribution necessarily goes over into a Wigner distribution under the phase space mirror reflection.

Following the notations of Duan et al. [30], the separability criterion expresses the fact that a two-mode separable state will obey the following inequality

$$\Delta \equiv \langle(\Delta\hat{u})^2\rangle + \langle(\Delta\hat{v})^2\rangle \geq \alpha^2 + \frac{1}{\alpha^2}, \tag{3.10}$$

where Δ is called the EPR variance, and for any real (non-zero) α the operators are

$$\hat{u} = |\alpha|\hat{x}_1 + \frac{1}{\alpha}\hat{x}_2, \tag{3.11}$$

$$\hat{v} = |\alpha|\hat{p}_1 - \frac{1}{\alpha}\hat{p}_2, \tag{3.12}$$

which are functions of the quadratures components $\hat{x}$ and $\hat{p}$ of modes 1 and 2. Therefore, if the state violates inequality for at least one value of α, it is entangled (3.10). The inequality (3.10) was derived without using the PPT criterion. In order to obtain this inequality by applying the PPT criterion, let's define a new operator as

$$\hat{v}' = |\alpha|\hat{p}_1 + \frac{1}{\alpha}\hat{p}_2. \tag{3.13}$$

For any two observable A and B, the Robertson uncertainty relation can be written as

$$\sigma_A^2\sigma_B^2 \geq \frac{1}{4}|\langle\psi[A, B]|\psi\rangle|^2, \tag{3.14}$$

where $[\cdot, \cdot]$ stands for the commutator. Obviously, if $A = x$ and $B = p$ we retrieve the Heisenberg uncertainty relation. From the Robertson uncertainty relation, we know that

every physical state must obey the following inequality

$$\sqrt{\langle(\Delta\hat{u})^2\rangle\langle(\Delta\hat{v}')^2\rangle} \geq \frac{1}{2}\left|\langle[\hat{u},\hat{v}']\rangle\right|^2 = \frac{1}{2}\left(\alpha^2+\frac{1}{\alpha^2}\right). \tag{3.15}$$

Using the inequality $x^2+y^2 \geq 2xy$, we obtain that any ρ satisfies

$$\left\langle\left(\Delta\hat{u}\right)_\rho^2\right\rangle + \left\langle\left(\Delta\hat{v}'\right)_\rho^2\right\rangle \geq 2\sqrt{\left\langle\left(\Delta\hat{u}\right)_\rho^2\right\rangle\left\langle\left(\Delta\hat{v}'\right)_\rho^2\right\rangle} \geq \alpha^2+\frac{1}{\alpha^2}. \tag{3.16}$$

We can now make use of the PPT criterion. If a state ρ is separable, then its partial transposed state ρ^{PT} must also be physical and so, it must verify the same inequality

$$\left\langle\left(\Delta\hat{u}\right)_{\rho^{PT}}^2\right\rangle + \left\langle\left(\Delta\hat{v}'\right)_{\rho^{PT}}^2\right\rangle \geq \alpha^2+\frac{1}{\alpha^2}. \tag{3.17}$$

The partial transpose on the second mode simply means that $\hat{p}_2$ goes to $-\hat{p}_2$. Therefore, we have $\left\langle\left(\Delta\hat{u}\right)_{\rho^{PT}}^2\right\rangle = \left\langle\left(\Delta\hat{u}\right)_\rho^2\right\rangle$ and $\left\langle\left(\Delta\hat{v}'\right)_{\rho^{PT}}^2\right\rangle = \left\langle\left(\Delta\hat{v}\right)_\rho^2\right\rangle$, which yields the same result as (3.10). Remarkably, in the case of Gaussian states, this separability condition becomes necessary and sufficient. One can show that every covariance matrix of a Gaussian state can be transformed by symplectic transformations into the standard form

$$\xi = \begin{bmatrix} n_1 & 0 & c_1 & 0 \\ 0 & n_2 & 0 & c_2 \\ c_1 & 0 & m_1 & 0 \\ 0 & c_2 & 0 & m_2 \end{bmatrix}, \tag{3.18}$$

where

$$\frac{n_1-1}{m_1-1} = \frac{n_2-1}{m_2-1}$$

and

$$|c_1|-|c_2| = \sqrt{(n_1-1)(m_1-1)}-\sqrt{(n_2-1)(m_2-1)}.$$

Introducing the following operators related to the covariance matrix ξ

$$\hat{u}'' = \alpha_0\hat{x}_1 - \frac{c_1}{|c_1|}\frac{1}{\alpha_0}\hat{x}_2, \tag{3.19}$$

$$\hat{v}'' = \alpha_0\hat{p}_1 - \frac{c_2}{|c_2|}\frac{1}{\alpha_0}\hat{p}_2, \tag{3.20}$$

where

$$\alpha_0^2 = \sqrt{\frac{m_1 - 1}{n_1 - 1}} = \sqrt{\frac{m_2 - 1}{n_2 - 1}}. \tag{3.21}$$

So a necessary and sufficient separability criterion can be expressed as: a Gaussian state is separable if and only if

$$\Delta \geq \alpha_0^2 + \frac{1}{\alpha_0^2},$$

where Δ is defined in equation (3.10). This implies that

$$\alpha_0^2\Big(\frac{n_1 + n_2}{2}\Big) + \Big(\frac{m_1 + m_2}{2\alpha_0^2}\Big) - |c_1| - |c_2| \geq \alpha_0^2 + \frac{1}{\alpha_0^2}. \tag{3.22}$$

Furthermore, it is also possible to obtain Mancini separability criterion [29] from equation (3.15) by using again that $\Big\langle \big(\Delta\hat{u}\big)^2_{\rho^{PT}} \Big\rangle = \Big\langle \big(\Delta\hat{u}\big)^2_{\rho} \Big\rangle$ and $\Big\langle \big(\Delta\hat{v}'\big)^2_{\rho^{PT}} \Big\rangle = \Big\langle \big(\Delta\hat{v}\big)^2_{\rho} \Big\rangle$. After a partial transposition we can write that any separable state must respect the inequality

$$\Delta' \equiv 2\sqrt{\big\langle (\Delta\hat{u})^2_{\rho} \big\rangle \big\langle (\Delta\hat{v})^2_{\rho} \big\rangle} \geq \alpha^2 + \frac{1}{\alpha^2}. \tag{3.23}$$

According to Equation (3.16), this criterion is stronger than the Duan et al. criterion [30]. Although, both criteria must coincide for Gaussian states since the Duan-Simon criterion is necessary and sufficient in this case. To see this, let us take a Gaussian state. The state is entangled if $\Delta' < \alpha^2 + \frac{1}{\alpha^2}$. On the other hand if $\Delta' \geq \alpha^2 + \frac{1}{\alpha^2}$, according to equation (3.16) , we can also say that the sum of the variances Δ is greater than $\alpha^2 + \frac{1}{\alpha^2}$. For Gaussian states, we showed that $\Delta \geq \alpha^2 + \frac{1}{\alpha^2}$ means that the state is separable (see equation (3.22). Condition (3.23) is thus necessary and sufficient for Gaussian states.

3.3 Non-Gaussian Entanglement Criterion

Entanglement has proven to be an important resource in quantum information processing. However, determining whether a state is entangled or not is often far from simple. In particular, for systems with continuous degrees of freedom, such as particle position or momentum or the quadrature components of field modes, the number of available criteria

for detecting entanglement is very limited. In addition, each of the known criteria detects only a subset of the set of entangled states. In many cases, these criteria are in the form of inequalities.

Entanglement criteria for non-Gaussian states are explored in references [40, 41]. The underlying principle of both criteria is uncertainty principles. They constructed a specific form of operators and demonstrated uncertainty principle for these operators to figure out the necessary condition for the separability of states, which is an equivalent condition of entanglement.

3.3.1 H-Z criteria

Hillery and Zubairy criteria provided a class of inequalities whose violation shows the presence of entanglement in two-mode systems. They initially consider observables that are quadratic in the mode creation and annihilation operators and find conditions under which a two-mode state is entangled. This criterion is based on comparing between two inequalities, one is derived to be satisfied by every physical state while the other one is a necessary condition that every separable state needs to fulfill. Thus, a sufficient condition for a state to be entangled is obtained when the first condition is satisfied while the second is violated. The criteria for both groups of operators are separately described below.

Hillery and Zubairy constructed two sets of operators. The first set of operators obeys $SU(2)$ algebra and it is related to the interaction between two quantum systems. $SU(2)$ are spin like operators (Pauli matrices). The second set of operators satisfies $SU(1,1)$ algebra and is related to the non-linear parametric generation and conversion of two photons.

Considering first SU(2) operators. Assume $L_1 = ab^\dagger + a^\dagger b$, $L_2 = i(ab^\dagger - a^\dagger b)$ and $L_3 = a^\dagger a + b^\dagger b$ are SU(2) operators with $a^\dagger$ and $b^\dagger$ denotes creation operator associated with different modes a and b. The commutation relation between these operators is

$[J_i, J_j] = i\epsilon_{ijk}J_k$, where $J_i = L_i/2$. The variance of these operators is

$$(\Delta L_i)^2 = \langle (L_i)^2 \rangle - \langle L_i \rangle^2 \qquad i = 1, 2. \tag{3.24}$$

Using definition of L_1 and L_2, and $N_a = a^\dagger a$ $N_b = b^\dagger b$ we obtained

$$(\Delta L_1)^2 + (\Delta L_2)^2 = 2[\langle (N_a + 1)N_b \rangle + \langle N_a(N_b + 1) \rangle - 2|\langle ab^\dagger \rangle^2]. \tag{3.25}$$

For separable sate we can express that N_a and N_b are not correlated

$$(\Delta L_1)^2 + (\Delta L_2)^2 = 2[\langle (N_a + 1) \rangle \langle N_b \rangle + \langle N_a \rangle \langle (N_b + 1) \rangle - 2|\langle a \rangle \langle b^\dagger \rangle^2]. \tag{3.26}$$

Using Cauchy-Schwarz inequality

$$|\langle x, y \rangle|^2 \leq \langle x, x \rangle \langle y, y \rangle.$$

Suppose x=a and y=1 we get $|\langle a \rangle|^2 \leq \langle a, a \rangle = \langle N_a \rangle$ and for b we get $|\langle b \rangle|^2 \leq \langle N_b \rangle$. The equation (3.25) can give a separable condition for states given by

$$(\Delta L_1)^2 + (\Delta L_2)^2 \geq 2(\langle N_a \rangle + \langle N_b \rangle). \tag{3.27}$$

Finding a separable condition for all states. As density matrix of a separable state can be written as, $\rho = \sum_n p_n \rho_n^A \otimes \rho_n^B$. Calculating variance of an observable A for ρ

$$(\Delta A)^2 = tr(\rho A^2) - [tr(\rho A)]^2 \geq \sum_n p_n [\Delta A_n]^2.$$

The inequality became an equation if the expectation value of A with respect to each state is vanished. This shows that the variance of any observable calculated with respect to the overall system density matrix of a separable state can never be less than the summation of the variance of individual subsystems.

Next, considering the uncertaity relation $(\Delta L_1)(\Delta L_2) \geq \frac{1}{2i}|\langle [L_1, L_2] \rangle|$ and using commutation relation we get $(\Delta L_1)(\Delta L_2) \geq |\langle N_a - N_b \rangle|$. This can give further relation written as

$$(\Delta L_1 - \Delta L_2)^2 \geq 0 \implies (\Delta L_1)^2 + (\Delta L_2)^2 \geq (\Delta L_1)(\Delta L_2)(\Delta L_2)(\Delta L_1),$$

$$(\Delta L_1)^2 + (\Delta L_2)^2 \geq 2|\langle N_a - N_b \rangle|. \tag{3.28}$$

Every physical state will satisfy inequality (3.28). States which satisfy inequality (3.28) but fail to satisfy (3.27) are considered entangled. These two inequalities are necessary condition for separable states and sufficient condition for entangled states.

Next suppose that M_1, M_2 and M_3 are $SU(1,1)$ operators which satisfy $SU(1,1)$ algebra. These operators can be written as , $M_1 = ab + a^\dagger b^\dagger$, $M_2 = i(a^\dagger b^\dagger - ab)$ and $M_3 = a^\dagger a - b^\dagger b$. Let M be a new operator which depends on the phase and can be represented as

$$M(\phi) = e^{i\phi} a^\dagger b^\dagger + e^{-i\phi} ab. \tag{3.29}$$

This operator becomes M_1 when $\phi = 0$ and become M_2 when $\phi = \pi/2$. It is proved in [40] that states are separable if $(\Delta M(\phi)) \geq 1$ and entangled if $(\Delta M(\phi)) < 1$.

Considering an example associated to a product state in order to obtain inequalities of this class

$$|\langle ab \rangle| = |\langle a \rangle \langle b \rangle| \leq [\langle a^\dagger a \rangle \langle b^\dagger b \rangle]^{1/2},$$

$$|\langle ab \rangle| \leq [\langle N_a \rangle \langle N_b \rangle]^{1/2}. \tag{3.30}$$

Generally we can write for separable states as

$$|\langle a^m b^n \rangle| \leq [\langle (a^\dagger)^m a^m \rangle \langle (b^\dagger)^n b^n \rangle]^{1/2}.$$

For m=n=1 we get

$$|\langle ab \rangle| \leq [\langle N_a + 1 \rangle \langle N_b + 1 \rangle]^{1/2}. \tag{3.31}$$

Every physcial state satisfy inequality (3.31). A state that satisfy (3.31) but violates the inequality (3.30) will be entangled state. These inequalities provides another sufficient condition to identify entanglement. In addition, we can say that an entangled state stasify $[\langle N_a \rangle \langle N_b \rangle]^{1/2} < |\langle ab \rangle|$.

3.3.2 NZ Criteria

Nha and Zubairy demonstrated a sufficient condition of entanglement and obtained an inequality relation by using Schrodinger-Robertson inequality instead of using the Cauchy-Schwarz inequality [41] utilized in the previous subsection. The Schrodinger-Robertson uncertainty relation for two operators, say A and B, can be expressed as

$$\langle(\Delta A)^2\rangle\langle(\Delta B)^2\rangle \geq \frac{1}{4}|[A,B]|^2 + \frac{1}{4}\langle\Delta A\Delta B\rangle_s^2. \tag{3.32}$$

SR inequality becomes traditional Heisenberg inequality when $\langle\Delta A\Delta B\rangle_s \equiv \langle\Delta A + \Delta B + \Delta B\Delta A\rangle$ vanish.

Another inequality was obtained through partial transpose operation, which is equivalent to the reflection of the second quadrature operator corresponding of the second subsystem. They determine a sufficient condition of entanglement as, for separable state both inequality should be satisfied, and if any of these inequality is violated the state will be entangled. In order to get the inequality, they constructed two sets of quadrature operators as

$$X_i^{(m)} \equiv a_i^{\dagger m} + a_i^m, \qquad and \qquad Y_i^{(m)} \equiv -i(a_i^{\dagger m} - a_i^m) \qquad i = 1, 2.$$

Let H_i be an Hermitian operator which is obtained through quadrature operators as

$$H_1 = X_1^{(m)} + X_2^{(n)} \qquad and \quad H_2 = Y_1^{(m)} + Y_2^{(n)}.$$

In the form of SR inequality, a separable condition can be expressed as

$$\Delta^2 H_1 \Delta^2 \tilde{H}_2 \geq \langle C_1^{(m)} + C_2^{(n)}\rangle^2 + \langle\Delta H_1 \Delta \tilde{H}_2\rangle_s^2, \tag{3.33}$$

where $C_1^{(m)} \equiv [a_i^m, a_i^{\dagger m}]$ and $\tilde{H}_2 \equiv Y_l^m - Y_2^{(n)}$. This form of $\tilde{H}_2$ is equivalent to the reflection of momentum on phase space which is the result of partial-transpose operation acting on the density matrix.

Considering another set of operators

$$X_{mn} \equiv a_1^{\dagger m} a_2^n + a_1^m a_2^{\dagger n} \quad and \quad Y_{mn} \equiv -i(a_1^{\dagger m} a_2^n - a_1^m a_2^{\dagger n}),$$

which again provide Hermitian operators as follows

$$H_1 = a_1^{\dagger m} a_2^{\dagger n} + a_1^m a_2^n \qquad and \qquad H_2 = -i(a_1^{\dagger m} a_2^{\dagger n} - a_1^m a_2^n).$$

The inequality provided by these operators is

$$(\Delta^2 X_{mn} + \langle C_1^{(m)} C_2^{(n)} \rangle)(\Delta^2 Y_{mn} + \langle C_1^{(m)} C_2^{(n)} \rangle) \geq \langle [a_1^m a_2^n, a_1^{\dagger m} a_2^{\dagger n}] \rangle^2 + \langle \Delta X_{mn} \Delta Y_{mn} \rangle_S^2 \quad (3.34)$$

The above two inequalities are very promising and important. Criteria demonstrated in articles are considered its special cases [42, 43]. Shchukin and Vogel proposed an experimental scheme for verification of these criteria [44].

3.4 Characteristic Function Criteria

Characteristic function $\tilde{\Phi}(\lambda_p)$ in (2.50) and $\Phi(\lambda_x)$ in (2.53) describes the self-correlation of the conjugate variables respectively. As a quantum system can't be perfectly located in position and momentum simultaneously, one would expect that there should exist some constraints on these functions in terms of quantum mechanical uncertainty relation. From their self-correlation forms as in equations (2.48) and (2.51), we can say that these functions naturally obey

$$|\Phi(\lambda_x)| \leq 1 \qquad and \qquad |\tilde{\Phi}(\lambda_p)| \leq 1, \quad (3.35)$$

so that we have a trivall relation as

$$|\Phi(\lambda_x)|^2 + |\tilde{\Phi}(\lambda_p)|^2 \leq 2. \quad (3.36)$$

Non-trivial relation was demonstrated in [10]

$$|\Phi(\lambda_x)|^2 + |\tilde{\Phi}(\lambda_p)|^2 \leq \beta(\lambda_x \lambda_p), \quad (3.37)$$

where

$$\beta(\gamma) = 2\sqrt{2} \frac{\sqrt{2} - \sqrt{1 - cos(\gamma)}}{1 + cos(\gamma)}. \quad (3.38)$$

Equation (3.38) oscillates periodically between the value 1 and 2. This relation is valid for all states, including mixed states and can be generalized to multidimensional contexts. It's strange that the uncertainty relation in equation (3.37) has an upper limit despite of the limit lower than other relations of uncertainty. The upper limit is attained by a normalized from the Dirac comb with a period of $2\pi/\lambda$, which is a non-Gaussian state. We can extend the treatment to a two-photon state $\hat{\rho}$, if we consider the characteristic functions as

$$\Phi_{\pm}(\lambda_x) = \langle e^{i\lambda_x \hat{x}_{\pm}} \rangle_{\hat{\rho}}, \tag{3.39}$$

$$\tilde{\Phi}_{\pm}(\lambda_p) = \langle e^{i\lambda_p \hat{p}_{\pm}} \rangle_{\hat{\rho}}, \tag{3.40}$$

where $\mathbf{x}_i$ with $i = 1, 2$, is position of the i photon and $\mathbf{p}_i$ represents the momentum of i photon. Also assume that $[\mathbf{x}_j, \mathbf{p}_k] = i\delta_{j,k}$ and $j, k = 1, 2$. In the case of transverse spatially entangled photons, the position and momentum observables correspond to measurements in the near and in the far-field respectively, relative to the source plane, namely the SPDC crystal. The far field is associated with a momentum measurement at the source plane while the near field is associated with a position measurement at the source plane. Characteristic functions involving non-local operators and inequality (3.37) lead us to new entanglement criteria of spatial variables that is based on polarization measurement.

Chapter 4

Experiment

In this chapter, we will briefly present a proposal for direct measurement of the characteristic marginal distributions of the global spatial variables of photon pairs. Further, we will show how to use setup to test relations of uncertainty. This is interesting because the states that saturate it are not gaussian. Furthermore, it is possible to use this relation to establish new entanglement criteria from polarization measurements.

4.1 Experimental Proposal

In this section, we present an experimental proposal to obtain the characteristic functions of the spatial state of two photons. The experiment that we performed to obtain these characteristic functions is briefly explain below.

The experimental setup is shown in figure 4.1. A 325nm He-Cd laser (after passing through a filter to remove unwanted background fluorescence) pumps two crossed-axis, relatively thin, BBO crystals operated with type-I phase matching, producing polarization and spatially entangled photons through SPDC. The entangled photons have a degenerate wavelength of 650nm. The polarization direction of the pump beam is adjusted by HWP1. With a horizontally polarized pump beam (HWP1 = $-8°$) the down-conversion will only occur in the first crystal and the resulting down-conversion cone will be vertically polarized. Similarly, if the pump beam is vertically polarized (HWP1 = $37°$), the down-

conversion will occur in the second crystal and we obtain horizontally polarized photons. A diagonally polarized pump beam (HWP1 = 14°) will be equally likely to down convert in either crystal (neglecting losses from passing through the first) and these two possible down-conversion processes are coherent with one another, as long as the emitted spatial modes for a given pair of photons are indistinguishable for the two crystals. In our setup this happens naturally because the pump laser has a coherence length much larger than the crystal length, the state of the twin photons is described as

$$|\Psi^{(2)}\rangle = |\Phi^{+}\rangle \otimes |\psi^{(2)}\rangle,$$

where $|\psi^{(2)}\rangle$ stands for the spatial degree of freedom of the twin photon, and $|\Phi^{+}\rangle = \big(|HH\rangle + |VV\rangle\big)/\sqrt{2}$ is the polarization state. H (V) stands for horizontal (vertical) polarization. The twin photons obtained by SPDC shows a large amount of spatial entanglement, that appears in the form of correlation in the near field, and anti-correlation in the far field. A pair of lenses (not shown) is used to map the source plane onto mirror M1. The amount of correlations in these variables depends on the configuration of the pump beam.

A dichroic mirror (DM) is used to separate the down-converted photons from the pump laser. After passing through adjustable irises both photons are sent into a Sagnac interferometer, which serves to apply a controlled displacement in the beam of twin photons. The incident beam is separated by a polarizing beam splitter into its horizontal and vertical components. The H-polarized (V-polarized) photons propagate in the clock-wise (anti-clock-wise) direction in the interferometer. These components are coherently combined in the same PBS. A slight misalignment of the intermediate mirror of the interferometer mirror (M1) implements a controlled displacement in the beam. Hence the twin photons undergo a unitary evolution by passing through Sagnac interferometer, which is given as [45]

$$\hat{U}_j = |H\rangle_j\langle H|_j \otimes e^{-i\frac{\lambda_x}{2}\hat{x}_j} + |V\rangle_j\langle V|_j \otimes e^{i\frac{\lambda_x}{2}\hat{x}_j} \qquad j = 1, 2. \tag{4.1}$$

This equation means that the $\hat{U}$ applies a transverse kick in the state, whose direction depends on the photon polarization. The parameter λ_x describes the effect of the tilted mirror (M1) of the interferometer and operator x_j is the transverse position of the photon j in the paraxial approximation. A stepper motor and a piezo-electric activator controlled the small angular deflections θ of M1.

The two-photon state evolve according to the non-local operator

$$\hat{U} = \hat{U}_1 \otimes \hat{U}_2. \tag{4.2}$$

A quarter wave-plate and half wave-plate in conjunction with a polarizing beam splitter are used to project onto different polarization states. Photons are detected and coincidence counts are registered. Note that we obtain a coincidence when both photons of a pair are detected, each of these detectors are equipped with a 8mm diameter circular aperture and a 10nm bandwidth filter centered at 650 nm. The detectors are connected to an electronic system that counts these coincidences.

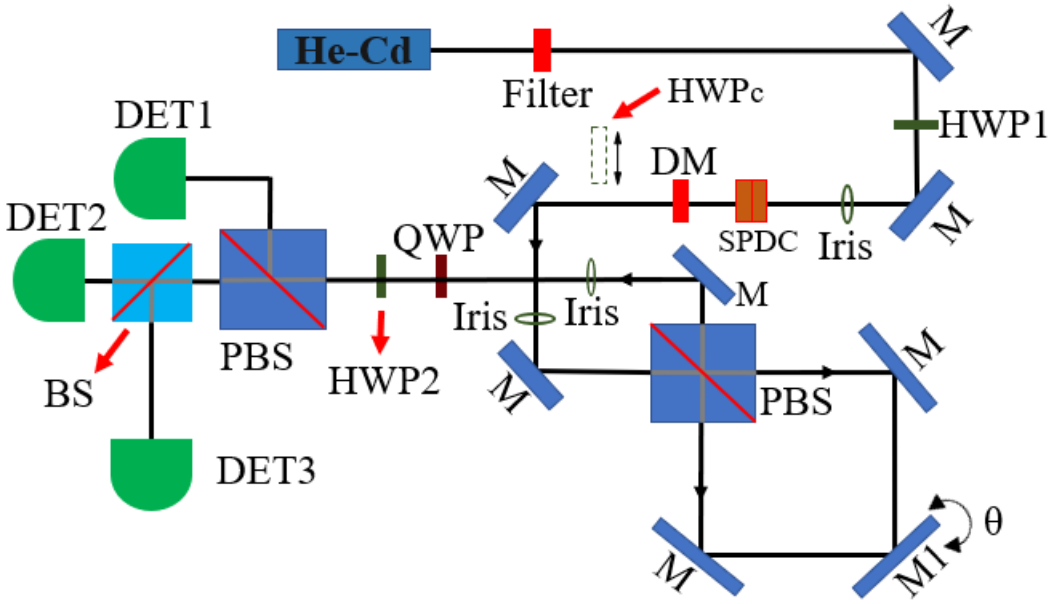

Fig. 4.1: Experimental setup (see text).

Considering two-photon state $\hat{\rho}$, the characteristic functions in terms of the spatial variables can be written as

$$\Phi_{\pm}(\lambda_x) = \langle e^{i\lambda_x \hat{x}_{\pm}} \rangle_{\hat{\rho}}, \tag{4.3}$$

$$\tilde{\Phi}_{\pm}(\lambda_p) = \langle e^{i\lambda_p \hat{p}_{\pm}} \rangle_{\hat{\rho}}, \tag{4.4}$$

Where the global operators for the spatial degrees of freedom of photon pairs can be written as

$$\mathbf{X}_{\pm} = \mathbf{x}_1 \pm \mathbf{x}_2, \tag{4.5}$$

$$\mathbf{P}_{\pm} = \mathbf{p}_1 \pm \mathbf{p}_2, \tag{4.6}$$

where $\mathbf{x}_i$ with $i = 1, 2$, is position of the i photon and $\mathbf{p}_i$ is momentum of i photon. These are non-local operators of the two photons with the characteristic functions in equation (4.5) and (4.6) and the inequality (3.37) is criterion for non-gaussian entanglement.

4.2 Theoretical model of experiment

In this section, we describe theoretically the experiment in figure 4.1 and show how the characteristic functions can be measured in this setup. For this, we use previous results obtained by an old PHD student of the lab [Eduardo's Thesis]. We found issues in this calculations that were corrected in this dissertation. Let's consider a two photon source based on SPDC like the one in reference [20] and presented in 4.1 section. A laser pumps a BBO crystals producing pairs of photons entangled in the polarization whose initial state is given by

$$\hat{\sigma_0} = |\Phi^-\rangle\langle\Phi^-| \otimes \hat{\rho}, \tag{4.7}$$

where

$$|\Phi^-\rangle = \frac{|HH\rangle - |VV\rangle}{\sqrt{2}}, \tag{4.8}$$

is the polarization state and $\hat{\rho}$ is the spatial degree of freedom of the twin photons. The twin photons will undergo a unitary evolution by passing through Sagnac interferometer

and the twin photon state will evolve according to the non-local operator in equation (4.2). The reduced state of polarization can be written as

$$\hat{\sigma}_{pol} = tr_{\hat{\rho}}(\hat{\sigma}). \tag{4.9}$$

Given that the state in equation (4.7) does not have terms with polarization $|HV\rangle$ or $|VH\rangle$, the evolved state is calculated as

$$\hat{\sigma} = \hat{U}\hat{\sigma}_0\hat{U}^{\dagger},$$

where

$$\hat{U} = |HH\rangle\langle HH| \otimes e^{-i\frac{\lambda_x}{2}\hat{x}_+} + |VV\rangle\langle VV| \otimes e^{i\frac{\lambda_x}{2}\hat{x}_+}.$$

The resulting state is

$$\hat{\sigma} = \frac{1}{2}\Big[|HH\rangle\langle HH| - |HH\rangle\langle VV| \otimes e^{-i\lambda_x\hat{x}_+} - |VV\rangle\langle HH| \otimes e^{i\lambda_x\hat{x}_+} + |VV\rangle\langle VV|\Big] \otimes \hat{\rho},$$

whose reduced state of polarization results in

$$\hat{\sigma}_{pol} = \frac{1}{2}\Big[|HH\rangle\langle HH| + |VV\rangle\langle VV| - (|HH\rangle\langle VV|\langle e^{-i\lambda_x\hat{x}_+}\rangle_{\hat{\rho}} + |VV\rangle\langle HH|\langle e^{i\lambda_x\hat{x}_+}\rangle_{\hat{\rho}})\Big]. \tag{4.10}$$

As can be seen from the experimental figure 4.1, we only can perform projective measurements where the state of each photon is projected onto orthogonal states. By projecting onto a state in the equator of the Bloch sphere given by

$$|\theta_{\pm}\rangle = \frac{|H\rangle \pm e^{i\theta}|V\rangle}{\sqrt{2}}, \tag{4.11}$$

the probability of observing coincidentally the photon 1 in $|\theta_+\rangle$ and a photon 2 in $|\theta_-\rangle$ is given by

$$p^{\hat{\rho},\theta}_{+-}(\lambda_x) = tr[|\theta_+\theta_-\rangle\langle\theta_+\theta_-|\hat{\sigma}_{pol}] = \langle\theta_+\theta_-|\hat{\sigma}_{pol}|\theta_+\theta_-\rangle,$$

$$p^{\hat{\rho},\theta}_{+-}(\lambda_x) = \frac{1}{4}\Big[1 + \big\{cos(2\theta)\langle cos\lambda_x\hat{x}_+\rangle_{\hat{\rho}} + sin(2\theta)\langle sin\lambda_x\hat{x}_+\rangle_{\hat{\rho}}\big\}\Big], \tag{4.12}$$

$$p^{\hat{\rho},\theta}_{-+}(\lambda_x) = \langle\theta_-\theta_+|\hat{\sigma}_{pol}|\theta_-\theta_+\rangle,$$

$$p^{\hat{\rho},\theta}_{-+}(\lambda_x) = \frac{1}{4}\Big[1 + \big\{cos(2\theta)\langle cos\lambda_x\hat{x}_+\rangle_{\hat{\rho}} + sin(2\theta)\langle sin\lambda_x\hat{x}_+\rangle_{\hat{\rho}}\big\}\Big] = p^{\hat{\rho},\theta}_{+-}(\lambda_x), \tag{4.13}$$

$$p^{\hat{\rho},\theta}_{++}(\lambda_x) = \langle\theta_+\theta_+|\hat{\sigma}_{pol}|\theta_+\theta_+\rangle,$$

$$p^{\hat{\rho},\theta}_{++}(\lambda_x) = \frac{1}{4}\Big[1 - \big\{cos(2\theta)\langle cos\lambda_x\hat{x}_+\rangle_{\hat{\rho}} + sin(2\theta)\langle sin\lambda_x\hat{x}_+\rangle_{\hat{\rho}}\big\}\Big], \tag{4.14}$$

$$p^{\hat{\rho},\theta}_{--}(\lambda_x) = \langle\theta_-\theta_-|\hat{\sigma}_{pol}|\theta_-\theta_-\rangle,$$

$$p^{\hat{\rho},\theta}_{--}(\lambda_x) = \frac{1}{4}\Big[1 - \big\{cos(2\theta)\langle cos\lambda_x\hat{x}_+\rangle_{\hat{\rho}} + sin(2\theta)\langle sin\lambda_x\hat{x}_+\rangle_{\hat{\rho}}\big\}\Big] = p^{\hat{\rho},\theta}_{++}(\lambda_x). \tag{4.15}$$

According to the choice of θ we can get the expected value of sine and cosine. Moreover since the emission of the photons is collinear with the laser pump therefore we are restricted to use only two detectors common to both the photons, and hence we cannot individually obtain the values of $p^{\hat{\rho},\theta}_{+-}$ or $p^{\hat{\rho},\theta}_{-+}$.

Considering $\theta = 0$, we have

$$p^{\hat{\rho},0}_{+-}(\lambda_x) = \frac{1}{4}\Big[1 + \langle cos(\lambda_x\hat{x}_+)\rangle_{\hat{\rho}}\Big] = p^{\hat{\rho},0}_{-+}(\lambda_x),$$

$$p^{\hat{\rho},0}_{+-}(\lambda_x) + p^{\hat{\rho},0}_{-+}(\lambda_x) = \frac{1}{2}\Big[1 + \langle cos(\lambda_x\hat{x}_+)\rangle_{\hat{\rho}}\Big]. \tag{4.16}$$

If we consider $\theta = \pi/2$, then we have

$$p^{\hat{\rho},\pi/2}_{+-}(\lambda_x) + p^{\hat{\rho},\pi/2}_{-+}(\lambda_x) = \frac{1}{2}\Big[1 - \langle cos(\lambda_x\hat{x}_+)\rangle_{\hat{\rho}}\Big]. \tag{4.17}$$

To obtain the expected value of cosine, we subtract equation (4.17) from equation (4.16)

$$\langle cos(\lambda_x\hat{x}_+)\rangle_{\hat{\rho}} = \Big[p^{\hat{\rho},0}_{+-}(\lambda_x) + p^{\hat{\rho},0}_{-+}(\lambda_x)\Big] - \Big[p^{\hat{\rho},\pi/2}_{+-}(\lambda_x) + p^{\hat{\rho},\pi/2}_{-+}(\lambda_x)\Big]. \tag{4.18}$$

On the other hand, if we choose $\theta = \pi/4$ we obtain

$$p^{\hat{\rho},\pi/4}_{+-}(\lambda_x) = \frac{1}{4}\Big[1 + \langle sin(\lambda_x\hat{x}_+)\rangle_{\hat{\rho}}\Big] = p^{\hat{\rho},\pi/4}_{-+}(\lambda_x),$$

$$p^{\hat{\rho},\pi/4}_{+-}(\lambda_x) + p^{\hat{\rho},\pi/4}_{-+}(\lambda_x) = \frac{1}{2}\Big[1 + \langle sin(\lambda_x\hat{x}_+)\rangle_{\hat{\rho}}\Big]. \tag{4.19}$$

If we consider $\theta = -\pi/4$

$$p^{\hat{\rho},-\pi/4}_{+-}(\lambda_x) = \frac{1}{4}\Big[1 - \langle sin(\lambda_x\hat{x}_+)\rangle_{\hat{\rho}}\Big] = p^{\hat{\rho},-\pi/4}_{-+}(\lambda_x),$$

$$p_{+-}^{\hat{\rho},-\pi/4}(\lambda_x) + p_{-+}^{\hat{\rho},-\pi/4}(\lambda_x) = \frac{1}{2}\Big[1 - \langle sin(\lambda_x \hat{x}_+)\rangle_{\hat{\rho}}\Big]. \tag{4.20}$$

We can obtain the expectation value of sine by subtracting equation (4.20) from equation (4.19)

$$\langle sin(\lambda_x \hat{x}_+)\rangle_{\hat{\rho}} = \Big[p_{+-}^{\hat{\rho},\pi/4}(\lambda_x) + p_{-+}^{\hat{\rho},\pi/4}(\lambda_x)\Big] - \Big[p_{+-}^{\hat{\rho},-\pi/4}(\lambda_x) + p_{-+}^{\hat{\rho},-\pi/4}(\lambda_x)\Big] \tag{4.21}$$

Experimentally we are not measuring probabilities but measuring coincidence counts often projecting onto the basis $|\theta_\pm\rangle$. Consider that N is the total number of photon pairs, so we can calculate the coincidence counts from probability as $C_{+-}^{\hat{\rho},\theta} + C_{-+}^{\hat{\rho},\theta} = N(p_{+-}^{\hat{\rho},\theta} + p_{-+}^{\hat{\rho},\theta})$. Rewriting in term of coincidence counts, equation (4.18) and equation (4.21) can be result in

$$\langle cos(\lambda_x \hat{x}_+)\rangle_{\hat{\rho}} = \frac{\Big[C_{+-}^{\hat{\rho},0}(\lambda_x) + C_{-+}^{\hat{\rho},0}(\lambda_x)\Big] - \Big[C_{+-}^{\hat{\rho},\pi/2}(\lambda_x) + C_{-+}^{\hat{\rho},\pi/2}(\lambda_x)\Big]}{N}, \tag{4.22}$$

and

$$\langle sin(\lambda_x \hat{x}_+)\rangle_{\hat{\rho}} = \frac{\Big[C_{+-}^{\hat{\rho},\pi/4}(\lambda_x) + C_{-+}^{\hat{\rho},\pi/4}(\lambda_x)\Big] - \Big[C_{+-}^{\hat{\rho},-\pi/4}(\lambda_x) + C_{-+}^{\hat{\rho},-\pi/4}(\lambda_x)\Big]}{N}. \tag{4.23}$$

Considering $\lambda_x = 0$ in equation (4.22) we can obtain the value of N as

$$N = \Big[C_{+-}^{\hat{\rho},0}(0) + C_{-+}^{\hat{\rho},0}(0)\Big] - \Big[C_{+-}^{\hat{\rho},\pi/2}(0) + C_{-+}^{\hat{\rho},\pi/2}(0)\Big]. \tag{4.24}$$

If we substitute the value of N in equation (4.22) and (4.23) we obtain

$$\langle cos(\lambda_x \hat{x}_+)\rangle_{\hat{\rho}} = \frac{\Big[C_{+-}^{\hat{\rho},0}(\lambda_x) + C_{-+}^{\hat{\rho},0}(\lambda_x)\Big] - \Big[C_{+-}^{\hat{\rho},\pi/2}(\lambda_x) + C_{-+}^{\hat{\rho},\pi/2}(\lambda_x)\Big]}{\Big[C_{+-}^{\hat{\rho},0}(0) + C_{-+}^{\hat{\rho},0}(0)\Big] - \Big[C_{+-}^{\hat{\rho},\pi/2}(0) + C_{-+}^{\hat{\rho},\pi/2}(0)\Big]}, \tag{4.25}$$

$$\langle sin(\lambda_x \hat{x}_+)\rangle_{\hat{\rho}} = \frac{\Big[C_{+-}^{\hat{\rho},\pi/4}(\lambda_x) + C_{-+}^{\hat{\rho},\pi/4}(\lambda_x)\Big] - \Big[C_{+-}^{\hat{\rho},-\pi/4}(\lambda_x) + C_{-+}^{\hat{\rho},-\pi/4}(\lambda_x)\Big]}{\Big[C_{+-}^{\hat{\rho},0}(0) + C_{-+}^{\hat{\rho},0}(0)\Big] - \Big[C_{+-}^{\hat{\rho},\pi/2}(0) + C_{-+}^{\hat{\rho},\pi/2}(0)\Big]}. \tag{4.26}$$

With these results one can obtain the expected value of the characteristic function in the state $\hat{\rho}$ as

$$\Phi_+(\lambda_x) = \langle e^{i\lambda_x \hat{x}_+}\rangle_{\hat{\rho}} = \langle cos(\lambda_x \hat{x}_+)\rangle_{\hat{\rho}} + i\langle sin(\lambda_x \hat{x}_+)\rangle_{\hat{\rho}}. \tag{4.27}$$

As $\hat{\rho}$ is the two-photon state in the intermediate mirror of the interferometer. However we are interested to find the expected value of this operator in the state of two-photon at position of the crystal, so we must use a set of lens system between the crystal and interferometer mirror. A Fourier optical system, which consists on one confocal lens that evolve the state of photon j with the unitary operator

$$\hat{F}_j^{\dagger}\hat{x}_j\hat{F}_j = \frac{f}{k}\hat{p}_j, \tag{4.28}$$

where f the represent focal length of the lens, k is the wavenumber of the electromagnetic field and $\hat{p}_j$ is the transverse momentum operator in the paraxial approximation. The global operator is given by the direct product from the local operators for the two modes $\hat{F} = \hat{F}_1 \otimes \hat{F}_2$. The expected value of the operator in state $\hat{\rho}'$, which is the state after the Fourier transformation ($\hat{\rho}' = \hat{F}\hat{\rho}\hat{F}^{\dagger}$) can be written as

$$\begin{aligned}
\langle e^{\pm i\lambda_x\hat{x}_+}\rangle_{\hat{\rho}} \rightarrow \langle e^{\pm i\lambda_x\hat{x}_+}\rangle_{\hat{\rho}'} &= tr\Big[\hat{\rho}' e^{\pm i\lambda_x\hat{x}_+}\Big], \\
= tr\Big[\hat{F}\hat{\rho}\hat{F}^{\dagger}e^{\pm i\lambda_x\hat{x}_+}\Big] &= tr\Big[\hat{\rho}\hat{F}^{\dagger}e^{\pm i\lambda_x\hat{x}_+}\hat{F}\Big], \\
tr\Big[\hat{\rho}e^{\pm i\lambda_x\frac{f}{k}\hat{p}_+}\Big] &= tr\Big[\hat{\rho}e^{\pm i\lambda_p\hat{p}_+}\Big], \\
\Longrightarrow \langle e^{\pm i\lambda_x\hat{x}_+}\rangle_{\hat{\rho}'} &= \langle e^{\pm i\lambda_p\hat{p}_+}\rangle_{\hat{\rho}}.
\end{aligned} \tag{4.29}$$

Equation (4.29) implies that applying a linear phase to the momentum in a state $\hat{\rho}$ is equivalent to applying a linear phase with the position in the state $\hat{\rho}'$ transformed by Fourier optical system. It should be also noted that the experimental parameter which we have a direct control is λ_x. To convert from λ_p to λ_x we must use a rescaling factor k/f. Finally we can write as

$$\tilde{\Phi}_+(\lambda_p) = \langle e^{i\lambda_p\hat{p}_+}\rangle_{\hat{\rho}} = \langle cos(\lambda_p\hat{p}_+)\rangle_{\hat{\rho}} + i\langle sin(\lambda_p\hat{p}_+)\rangle_{\hat{\rho}}, \tag{4.30}$$

where

$$\langle cos(\lambda_p\hat{p}_+)\rangle_{\hat{\rho}} = \frac{\Big[C_{+-}^{\hat{\rho}',0}(\lambda_x) + C_{-+}^{\hat{\rho}',0}(\lambda_x)\Big] - \Big[C_{+-}^{\hat{\rho}',\pi/2}(\lambda_x) + C_{-+}^{\hat{\rho}',\pi/2}(\lambda_x)\Big]}{\nu}, \tag{4.31}$$

$$\langle sin(\lambda_p\hat{p}_+)\rangle_{\hat{\rho}} = \frac{\Big[C_{+-}^{\hat{\rho}',\pi/4}(\lambda_x) + C_{-+}^{\hat{\rho}',\pi/4}(\lambda_x)\Big] - \Big[C_{+-}^{\hat{\rho}',-\pi/4}(\lambda_x) + C_{-+}^{\hat{\rho}',-\pi/4}(\lambda_x)\Big]}{\nu}, \tag{4.32}$$

and

$$\nu = \Big[C_{+-}^{\hat{\rho}',0}(0) + C_{-+}^{\hat{\rho}',0}(0)\Big] - \Big[C_{+-}^{\hat{\rho}',\pi/2}(0) + C_{-+}^{\hat{\rho}',\pi/2}(0)\Big]. \tag{4.33}$$

Consider now that we use an optical imaging system (for instance, a 4f configuration with two lenses) between the crystal and mirror, the evolved state will be written as

$$\hat{\rho}'' = \hat{F}\hat{F}\hat{\rho}\hat{F}^{\dagger}\hat{F}^{\dagger}. \tag{4.34}$$

The expected value in $\hat{\rho}''$ will be equal to

$$\langle e^{\pm i\lambda_x \hat{x}_+}\rangle_{\hat{\rho}} \rightarrow \langle e^{\pm i\lambda_x \hat{x}_+}\rangle_{\hat{\rho}''} = tr\Big[\hat{\rho}'' e^{\pm i\lambda_x \hat{x}_+}\Big],$$

$$= tr\Big[\hat{F}\hat{F}\hat{\rho}\hat{F}^{\dagger}\hat{F}^{\dagger}e^{\pm i\lambda_x \hat{x}_+}\Big] = tr\Big[\hat{\rho}\hat{F}^{\dagger}\hat{F}^{\dagger}e^{\pm i\lambda_x \hat{x}_+}\hat{F}\hat{F}\Big],$$

$$= tr\Big[\hat{\rho}\hat{F}^{\dagger}e^{\pm i\lambda_p \hat{p}_+}\hat{F}\Big] = tr\Big[\hat{\rho}e^{\mp\frac{k}{f} i\lambda_p \hat{x}_+}\Big] = tr\Big[\hat{\rho}e^{\mp i\lambda_x \hat{x_+}}\Big],$$

$$\Longrightarrow \langle e^{\pm i\lambda_x \hat{x}_+}\rangle_{\hat{\rho}''} = \langle e^{\mp i\lambda_x \hat{x}_+}\rangle_{\hat{\rho}}. \tag{4.35}$$

Equation (4.35) have just a sign difference in the exponent. This reflects a known fact that an inverted image is obtained by the 4f optical system. So we can write as

$$\Phi_+(\lambda_x) = \langle e^{i\lambda_x \hat{x}_+}\rangle_{\hat{\rho}} = \langle cos(\lambda_x \hat{x}_+)\rangle_{\hat{\rho}} + i\langle sin(\lambda_x \hat{x}_+)\rangle_{\hat{\rho}}, \tag{4.36}$$

where

$$\langle cos(\lambda_x \hat{x}_+)\rangle_{\hat{\rho}} = \frac{\Big[C_{+-}^{\hat{\rho}'',0}(-\lambda_x) + C_{-+}^{\hat{\rho}'',0}(-\lambda_x)\Big] - \Big[C_{+-}^{\hat{\rho}'',\pi/2}(-\lambda_x) + C_{-+}^{\hat{\rho}'',\pi/2}(-\lambda_x)\Big]}{\nu}, \tag{4.37}$$

$$\langle sin(\lambda_x \hat{x}_+)\rangle_{\hat{\rho}} = \frac{\Big[C_{+-}^{\hat{\rho}'',\pi/4}(-\lambda_x) + C_{-+}^{\hat{\rho}'',\pi/4}(-\lambda_x)\Big] - \Big[C_{+-}^{\hat{\rho}'',-\pi/4}(-\lambda_x) + C_{-+}^{\hat{\rho}'',-\pi/4}(-\lambda_x)\Big]}{\nu} \tag{4.38}$$

Here ν is given as

$$\nu = \Big[C_{+-}^{\hat{\rho}'',0}(0) + C_{-+}^{\hat{\rho}'',0}(0)\Big] - \Big[C_{+-}^{\hat{\rho}'',\pi/2}(0) + C_{-+}^{\hat{\rho}'',\pi/2}(0)\Big]. \tag{4.39}$$

Considering an initial state

$$\hat{\sigma}_0' = |\Psi^-\rangle\langle\Psi^-| \otimes \hat{\rho}, \tag{4.40}$$

where

$$|\Psi^-\rangle = \frac{|HV\rangle - |VH\rangle}{\sqrt{2}}. \tag{4.41}$$

The evolved state is written as

$$\hat{\sigma}' = \frac{1}{2}\Big[|HV\rangle\langle HV| - |HV\rangle\langle VH| \otimes e^{-i\lambda_x \hat{x}_-} - |VH\rangle\langle HV| \otimes e^{i\lambda_x \hat{x}_-} + |VH\rangle\langle VH|\Big] \otimes \hat{\rho},$$

whose reduced state of polarization yields

$$\hat{\sigma}'_{pol} = \frac{1}{2}\Big[|HV\rangle\langle HV| + |VH\rangle\langle VH| - |HV\rangle\langle VH|\langle e^{-i\lambda_x \hat{x}_-}\rangle_{\hat{\rho}} - |VH\rangle\langle HV|\langle e^{i\lambda_x \hat{x}_-}\rangle_{\hat{\rho}}\Big]. \tag{4.42}$$

Measuring the pair of photon in the basis $|\theta_\pm\rangle$ in equation (4.11), we obtain the detection probabilities as

$$p^{\hat{\rho}}_{+-}(\lambda_x) = \frac{1}{4}\Big[1 + \langle cos\lambda_x \hat{x}_-\rangle_{\hat{\rho}}\Big] = p^{\hat{\rho}}_{-+}(\lambda_x), \tag{4.43}$$

$$p^{\hat{\rho}}_{++}(\lambda_x) = \frac{1}{4}\Big[1 - \langle cos\lambda_x \hat{x}_-\rangle_{\hat{\rho}}\Big] = p^{\hat{\rho}}_{--}(\lambda_x). \tag{4.44}$$

The expected value of cosine can be obtained from the following expression

$$\langle cos(\lambda_x \hat{x}_-)\rangle_{\hat{\rho}} = \Big[p^{\hat{\rho}}_{+-}(\lambda_x) + p^{\hat{\rho}}_{-+}(\lambda_x)\Big] - \Big[p^{\hat{\rho}}_{++}(\lambda_x) + p^{\hat{\rho}}_{--}(\lambda_x)\Big]. \tag{4.45}$$

Characteristic function in term of expectation value can be written as

$$\Phi_-(\lambda_x) = \langle e^{i\lambda_x \hat{x}_-}\rangle_{\hat{\rho}} = \langle cos(\lambda_x \hat{x}_-)\rangle_{\hat{\rho}} + i\langle sin(\lambda_x \hat{x}_-)\rangle_{\hat{\rho}}, \tag{4.46}$$

where in this state the sine term is vanishing. One of the future goals of this project consist on finding an initial state such that, after performing measurements, the values of $\langle sin(\lambda_x \hat{x}_-)\rangle$ can be obtained.

From the previous calculations, we obtain the characteristic function given in equation (4.36) through polarization measurements, by existing entanglement in the degree of freedom of photon polarization. This scheme significantly reduces measurement complexity

which is important for detection entanglement in transversal spatial variables. However, the experimental states are never pure and we haven't study so far how the mixing of the states affects the proposed scheme. Considering that we can produce Bell states but with reduce coherences, let's follow the previous procedure but with the state

$$\hat{\sigma_0} \longrightarrow \hat{\Xi}_\delta = [(1-\delta)|\Phi^-\rangle\langle\Phi^-| + \delta\hat{\chi}] \otimes \hat{\rho}, \tag{4.47}$$

where $0 \leq \delta \leq 1$ and $\hat{\chi}$ is written as

$$\hat{\chi} = \frac{|HH\rangle\langle HH| + |VV\rangle\langle VV|}{2}. \tag{4.48}$$

The state $\hat{\Xi}_\delta$ is exactly a Bell state but with the coherence reduced by a factor of $(\frac{1-\delta}{2})$, and is written as

$$\hat{\Xi}_\delta = \frac{1}{2}\Big[|HH\rangle\langle HH| - |HH\rangle\langle VV| - |VV\rangle\langle HH| + |VV\rangle\langle VV| + \\ +\delta|HH\rangle\langle VV| + \delta|VV\rangle\langle HH|\Big] \otimes \hat{\rho}.$$

As the operators are linear, the calculation for contribution of $|\Phi^-\rangle$ is the same as before. We calculate the evolution through out the interferometer of the extra term $\hat{\chi}$

$$\hat{U}(\hat{\chi}\otimes\hat{\rho})\hat{U}^\dagger = \frac{|HH\rangle\langle HH| \otimes e^{-i\frac{\lambda_x}{2}\hat{x}_+}\hat{\rho}e^{i\frac{\lambda_x}{2}\hat{x}_+} + |VV\rangle\langle VV| \otimes e^{i\frac{\lambda_x}{2}\hat{x}_+}\hat{\rho}e^{-i\frac{\lambda_x}{2}\hat{x}_+}}{2}. \tag{4.49}$$

The reduced state of polarization

$$tr_{\hat{\rho}}[\hat{U}(\hat{\chi}\otimes\hat{\rho})\hat{U}^\dagger] = \frac{|HH\rangle\langle HH| + |VV\rangle\langle VV|}{2} = \hat{\chi}. \tag{4.50}$$

The detection probabilities at basis $|\theta_\pm\rangle$ will be

$$p_{+-}^{\hat{\chi}\otimes\hat{\rho}} = \langle\theta_+\theta_-|\hat{\chi}|\theta_+\theta_-\rangle = p_{-+}^{\hat{\chi}\otimes\hat{\rho}} = \langle\theta_-\theta_+|\hat{\chi}|\theta_-\theta_+\rangle = \frac{1}{4}, \tag{4.51}$$

$$p_{++}^{\hat{\chi}\otimes\hat{\rho}} = \langle\theta_+\theta_+|\hat{\chi}|\theta_+\theta_+\rangle = p_{--}^{\hat{\chi}\otimes\hat{\rho}} = \langle\theta_-\theta_-|\hat{\chi}|\theta_-\theta_-\rangle = \frac{1}{4}. \tag{4.52}$$

Adding this result to equations (4.12) and (4.14) and taking into account the weight $(1-\delta)$, we obtain the detection probabilities as

$$p_{+-}^{\hat{\rho},\theta}(\lambda_x) = (1-\delta)\frac{1}{4}\Big[1 + \big\{cos(2\theta)\langle cos\lambda_x\hat{x}_+\rangle_{\hat{\rho}} + sin(2\theta)\langle sin\lambda_x\hat{x}_+\rangle_{\hat{\rho}}\big\}\Big] + \delta\frac{1}{4},$$

$$p^{\hat{\rho},\theta}_{+-}(\lambda_x) = p^{\hat{\rho},\theta}_{-+}(\lambda_x) = \frac{1}{4}\Big[1 + (1-\delta)\big\{cos(2\theta)\langle cos\lambda_x\hat{x}_+\rangle_{\hat{\rho}} + sin(2\theta)\langle sin\lambda_x\hat{x}_+\rangle_{\hat{\rho}}\big\}\Big], \quad (4.53)$$

$$p^{\hat{\rho},\theta}_{++}(\lambda_x) = p^{\hat{\rho},\theta}_{--}(\lambda_x) = \frac{1}{4}\Big[1 - (1-\delta)\big\{cos(2\theta)\langle cos\lambda_x\hat{x}_+\rangle_{\hat{\rho}} + sin(2\theta)\langle sin\lambda_x\hat{x}_+\rangle_{\hat{\rho}}\big\}\Big]. \quad (4.54)$$

Similarly, in equation (4.24) $N \longrightarrow \nu = (1-\delta)N$. The expected value for sine and cosine will remain the same, independently of the purity of polarization state. Hence mixing of the state has no effect to obtain the characteristic functions.

We will now calculate how the mixing of the state affects the results in equation (4.46) of the characteristic function $\Phi_-(\lambda_x)$ and $\Phi_-(\lambda_p)$. For this it is necessary to analyze carefully how the state $|\Psi^+\rangle$ is produced and what would be its mixed state counterpart $\hat{G}$. The crossed-axis source of poalrization entanglement produce states in (4.48). To produce the state $\hat{G}$, we introduce a HWPc as shown in figure 4.1 at 22.5° such that $|H\rangle \longrightarrow |D\rangle$ and $|V\rangle \longrightarrow |A\rangle$, where

$$|D\rangle = \frac{|H\rangle + |V\rangle}{\sqrt{2}},$$

and

$$|A\rangle = \frac{|H\rangle - |V\rangle}{\sqrt{2}}.$$

As $|\Phi^-\rangle$ is given in equation (4.8), so by introducing the HWP $|\Phi^-\rangle\langle\Phi^-|$, this state transform as

$$|\Phi^-\rangle\langle\Phi^-| \longrightarrow \Big(\frac{|DD\rangle - |AA\rangle}{\sqrt{2}}\Big)\Big(\frac{\langle DD| - \langle AA|}{\sqrt{2}}\Big), \quad (4.55)$$

where

$$|DD\rangle = \frac{1}{2}\big[|HH\rangle + |HV\rangle + |VH\rangle + |VV\rangle\big], \quad (4.56)$$

and

$$|AA\rangle = \frac{1}{2}\big[|HH\rangle - |HV\rangle - |VH\rangle + |VV\rangle\big]. \quad (4.57)$$

Therefore the state obtained after the HWP introduced in (4.55) can be written as

$$\frac{1}{2}\Big[|DD\rangle\langle DD| - |DD\rangle\langle AA| - |AA\rangle\langle DD| + |AA\rangle\langle AA|\Big] =$$

$$= \frac{1}{2}\Big[|HV\rangle\langle HV| + |HV\rangle\langle VH| + |VH\rangle\langle HV| + |VH\rangle\langle VH|\Big] = |\Psi^+\rangle\langle\Psi^+|. \quad (4.58)$$

Similarlay, the term ($\hat{\chi}$) that come from the fact that the experimental state is mixed, are also transformed by the HWP, resulting in

$$\hat{\chi} = \frac{|HH\rangle\langle HH| + |VV\rangle\langle VV|}{2} \longrightarrow \hat{Y} = \frac{|DD\rangle\langle DD| + |AA\rangle\langle AA|}{2}. \tag{4.59}$$

Using (4.56) and (4.57) we can write

$$\hat{Y} = \frac{1}{2}\Big[|\Phi^+\rangle\langle\Phi^+| + |\Psi^+\rangle\langle\Psi^+|\Big]. \tag{4.60}$$

Therefore by introducing the HWP at diagonal the mixed state $\hat{G}$ is produced from a state $\hat{\Xi}$ (given in equation (4.47)), and is written as

$$\hat{G} = \Big[(1-\delta)|\Psi^+\rangle\langle\Psi^+| + \frac{\delta}{2}(|\Phi^+\rangle\langle\Phi^+| + |\Psi^+\rangle\langle\Psi^+|)\Big] \otimes \hat{\rho}. \tag{4.61}$$

Again, using that the transformation that the interferometer implements is linear, we will only calculate the probabilities of states $|\Psi^+\rangle$ and $|\Phi^+\rangle$.

Assuming an initial two-photon state given by

$$\hat{k_0} = |\Psi^+\rangle\langle\Psi^+| \otimes \hat{\rho}, \tag{4.62}$$

where

$$|\Psi^+\rangle = \frac{|HV\rangle + |VH\rangle}{\sqrt{2}}. \tag{4.63}$$

The evolved state is written as

$$\hat{k} = \frac{1}{2}\Big[|HV\rangle\langle HV| + |HV\rangle\langle VH| \otimes e^{-i\lambda_x\hat{x}_-} + |VH\rangle\langle HV| \otimes e^{i\lambda_x\hat{x}_-} + |VH\rangle\langle VH|\Big] \otimes \hat{\rho},$$

whose reduced state of polarization is

$$\hat{k}_{pol} = \frac{1}{2}\Big[|HV\rangle\langle HV| + |VH\rangle\langle VH| + |HV\rangle\langle VH|\langle e^{-i\lambda_x\hat{x}_-}\rangle_{\hat{\rho}} + |VH\rangle\langle HV|\langle e^{i\lambda_x\hat{x}_-}\rangle_{\hat{\rho}}\Big]. \tag{4.64}$$

Measuring the pair of photon in the basis $|\theta_\pm\rangle$ in equation (4.11). After evolution, the probability of observing coincidentally the photon 1 in $|\theta_+\rangle$ and a photon 2 in $|\theta_-\rangle$ is given by

$$p^{\hat{\rho}}_{+-}(\lambda_x) = \frac{1}{4}\Big[1 - \langle cos\lambda_x\hat{x}_-\rangle_{\hat{\rho}}\Big] = p^{\hat{\rho}}_{-+}(\lambda_x), \tag{4.65}$$

$$p^{\hat{\rho}}_{++}(\lambda_x) = \frac{1}{4}\Big[1 + \langle cos\lambda_x\hat{x}_-\rangle_{\hat{\rho}}\Big] = p^{\hat{\rho}}_{--}(\lambda_x). \tag{4.66}$$

The expected value of cosine can be obtained from the following expression

$$\langle cos(\lambda_x \hat{x}_-)\rangle_{\hat{\rho}} = \Big[p^{\hat{\rho}}_{++}(\lambda_x) + p^{\hat{\rho}}_{--}(\lambda_x)\Big] - \Big[p^{\hat{\rho}}_{+-}(\lambda_x) + p^{\hat{\rho}}_{-+}(\lambda_x)\Big], \tag{4.67}$$

while the expectation value of sine is again vanished for this state.

Next considering an initial two-photon state given as

$$\hat{J}_0 = |\Phi^+\rangle\langle\Phi^+| \otimes \hat{\rho}, \tag{4.68}$$

where

$$|\Phi^+\rangle = \frac{|HH\rangle + |VV\rangle}{\sqrt{2}}. \tag{4.69}$$

The evolved state is written as

$$\hat{J} = \frac{1}{2}\Big[|HH\rangle\langle HH| + |HH\rangle\langle VV| \otimes e^{-i\lambda_x \hat{x}_+} + |VV\rangle\langle HH| \otimes e^{i\lambda_x \hat{x}_+} + |VV\rangle\langle VV|\Big] \otimes \hat{\rho},$$

whose reduced state of polarization is

$$\hat{J}_{pol} = \frac{1}{2}\Big[|HH\rangle\langle HH| + |HH\rangle\langle VV|\langle e^{-i\lambda_x \hat{x}_+}\rangle_{\hat{\rho}} + |VV\rangle\langle HH|\langle e^{i\lambda_x \hat{x}_+}\rangle_{\hat{\rho}} + |VV\rangle\langle VV|\Big]. \tag{4.70}$$

Measuring the pair of photon in the basis $|\theta_\pm\rangle$ in equation (4.11). After evolution, the probability of observing coincidentally the photon 1 in $|\theta_+\rangle$ and a photon 2 in $|\theta_-\rangle$ is given by

$$p^{\hat{\rho},\theta}_{+-}(\lambda_x) = \frac{1}{4}[1 - \{cos(2\theta)\langle cos\lambda_x \hat{x}_+\rangle_{\hat{\rho}} + sin(2\theta)\langle sin\lambda_x \hat{x}_+\rangle_{\hat{\rho}}\}] = p^{\hat{\rho},\theta}_{-+}(\lambda_x), \tag{4.71}$$

$$p^{\hat{\rho},\theta}_{++}(\lambda_x) = \frac{1}{4}\Big[1 + \big\{cos(2\theta)\langle cos\lambda_x \hat{x}_+\rangle_{\hat{\rho}} + sin(2\theta)\langle sin\lambda_x \hat{x}_+\rangle_{\hat{\rho}}\big\}\Big] = p^{\hat{\rho},\theta}_{--}(\lambda_x). \tag{4.72}$$

Using the probabilities (4.65), (4.66), (4.71) and (4.72) that are obtained for states $|\Psi^+\rangle\langle\Psi^+|$ and $|\Phi^+\rangle\langle\Phi^+|$, we can write the probabilities of observing the twin photons in the state $\hat{G}$ as

$$p^{\hat{\rho},\theta}_{+-}(\lambda_x) = (1-\delta)\frac{1}{4}\Big[1 - \langle cos\lambda_x \hat{x}_-\rangle_{\hat{\rho}}\Big] + \frac{\delta}{2}\frac{1}{4}\Big[1 - cos(2\theta)\langle cos\lambda_x \hat{x}_+\rangle_{\hat{\rho}} -$$

$$-sin(2\theta)\langle sin\lambda_x \hat{x}_+\rangle_{\hat{\rho}} + 1 - \langle cos\lambda_x \hat{x}_-\rangle_{\hat{\rho}}\Big],$$

$$p^{\hat{\rho},\theta}_{+-}(\lambda_x) = p^{\hat{\rho},\theta}_{-+}(\lambda_x) = \frac{1}{4}\Big[\big(1 - \langle cos\lambda_x\hat{x}_-\rangle_{\hat{\rho}}\big) + \frac{\delta}{2}\big(\langle cos\lambda_x\hat{x}_-\rangle_{\hat{\rho}} -$$
$$- cos(2\theta)\langle cos\lambda_x\hat{x}_+\rangle_{\hat{\rho}} - sin(2\theta)\langle sin\lambda_x\hat{x}_+\rangle_{\hat{\rho}}\big)\Big] \tag{4.73}$$

and

$$p^{\hat{\rho},\theta}_{++}(\lambda_x) = (1-\delta)\frac{1}{4}\Big[1 + \langle cos\lambda_x\hat{x}_-\rangle_{\hat{\rho}}\Big] + \frac{\delta}{2}\frac{1}{4}\Big[\big\{1 + cos(2\theta)\langle cos\lambda_x\hat{x}_+\rangle_{\hat{\rho}} +$$
$$sin(2\theta)\langle sin\lambda_x\hat{x}_+\rangle_{\hat{\rho}}\big\} + \big\{1 + \langle cos\lambda_x\hat{x}_-\rangle_{\hat{\rho}}\big\}\Big],$$

$$p^{\hat{\rho},\theta}_{++}(\lambda_x) = p^{\hat{\rho},\theta}_{--}(\lambda_x) = \frac{1}{4}\Big[\big(1 + \langle cos\lambda_x\hat{x}_-\rangle_{\hat{\rho}}\big) - \frac{\delta}{2}\big\{\langle cos\lambda_x\hat{x}_-\rangle_{\hat{\rho}} -$$
$$- cos(2\theta)\langle cos\lambda_x\hat{x}_+\rangle_{\hat{\rho}} - sin(2\theta)\langle sin\lambda_x\hat{x}_+\rangle_{\hat{\rho}}\big)\big\}\Big] \tag{4.74}$$

For $\theta = 0$ and $\pi/2$ we can obtain the following equation from equation (4.73) as

$$\frac{\delta}{4}\Big[\langle cos(\lambda_x\hat{x}_+)\rangle_{\hat{\rho}} + \langle sin(\lambda_x\hat{x}_+)\rangle_{\hat{\rho}}\Big] = \Big[p^{\hat{\rho},\pi/2}_{+-}(\lambda_x) + p^{\hat{\rho},\pi/2}_{-+}(\lambda_x)\Big] - \Big[p^{\hat{\rho},0}_{+-}(\lambda_x) + p^{\hat{\rho},0}_{-+}(\lambda_x)\Big], \tag{4.75}$$

and from equation (4.74) we can write

$$\frac{\delta}{2}\Big[\langle cos(\lambda_x\hat{x}_+)\rangle_{\hat{\rho}}\Big] = \Big[p^{\hat{\rho},\pi/2}_{++}(\lambda_x) + p^{\hat{\rho},\pi/2}_{--}(\lambda_x)\Big] - \Big[p^{\hat{\rho},0}_{++}(\lambda_x) + p^{\hat{\rho},0}_{--}(\lambda_x)\Big]. \tag{4.76}$$

Similarly for $\theta = \pi/4$ and $-\pi/4$ we can write an equation obtained from equation (4.73) as

$$\frac{\delta}{4}\Big[\langle cos(\lambda_x\hat{x}_+)\rangle_{\hat{\rho}} + \langle sin(\lambda_x\hat{x}_+)\rangle_{\hat{\rho}}\Big] = \Big[p^{\hat{\rho},-\pi/4}_{+-}(\lambda_x) + p^{\hat{\rho},-\pi/4}_{-+}(\lambda_x)\Big] - \Big[p^{\hat{\rho},\pi/4}_{+-}(\lambda_x) + p^{\hat{\rho},\pi/4}_{-+}(\lambda_x)\Big], \tag{4.77}$$

and from equation (4.74) we can write

$$\frac{\delta}{2}\Big[\langle sin(\lambda_x\hat{x}_+)\rangle_{\hat{\rho}}\Big] = \Big[p^{\hat{\rho},-\pi/4}_{++}(\lambda_x) + p^{\hat{\rho},-\pi/4}_{--}(\lambda_x)\Big] - \Big[p^{\hat{\rho},\pi/4}_{++}(\lambda_x) + p^{\hat{\rho},\pi/4}_{--}(\lambda_x)\Big]. \tag{4.78}$$

Summation of all probabilities yield

$$p^{\hat{\rho},\theta}_{+-}(\lambda_x) + p^{\hat{\rho},\theta}_{-+}(\lambda_x) + p^{\hat{\rho},\theta}_{++}(\lambda_x) + p^{\hat{\rho},\theta}_{--}(\lambda_x) = 1. \tag{4.79}$$

4.3 Results

We measured characteristic marginal distributions of the global spatial variables of a pair of photons given in equations (4.73) and (4.74). Characteristic functions for two-photon state $\hat{\rho}$ can be expressed in term of spatial variables as

$$\Phi_{\pm}(\lambda_x) = \langle e^{i\lambda_x \hat{x}_{\pm}} \rangle_{\hat{\rho}} = \langle cos(\lambda_x \hat{x}_{\pm}) \rangle_{\hat{\rho}} + i \langle sin(\lambda_x \hat{x}_{\pm}) \rangle_{\hat{\rho}}, \tag{4.80}$$

$$\tilde{\Phi}_{\pm}(\lambda_p) = \langle e^{i\lambda_p \hat{p}_{\pm}} \rangle_{\hat{\rho}} = \langle cos(\lambda_p \hat{p}_{\pm}) \rangle_{\hat{\rho}} + i \langle sin(\lambda_p \hat{p}_{\pm}) \rangle_{\hat{\rho}}. \tag{4.81}$$

Uncertainty relation of the characteristic function can be expressed as

$$|\Phi_{\pm}(\lambda_x)|^2 + |\tilde{\Phi}_{\pm}(\lambda_p)|^2 \leq \beta(\lambda_x \lambda_p) \tag{4.82}$$

We used this setup to test relation of uncertainty. Violation of this inequality identify entanglement in the states.

4.3.1 Experimental results

The preliminaries results obtained in our measurements are presented in the following figures. First we created a state given in equation (4.47). Then we give a sweep to motor closed to the region where we have the interference and measured projection onto $|DA\rangle$ (Black) and $|DD\rangle$ (Red), as shown in figure 4.2. In figure 4.2 measurement **a** corresponds to fourier for this state while the plot **b** corresponds to the measurment of image of state which is obtained by putting lenses after the crystals.

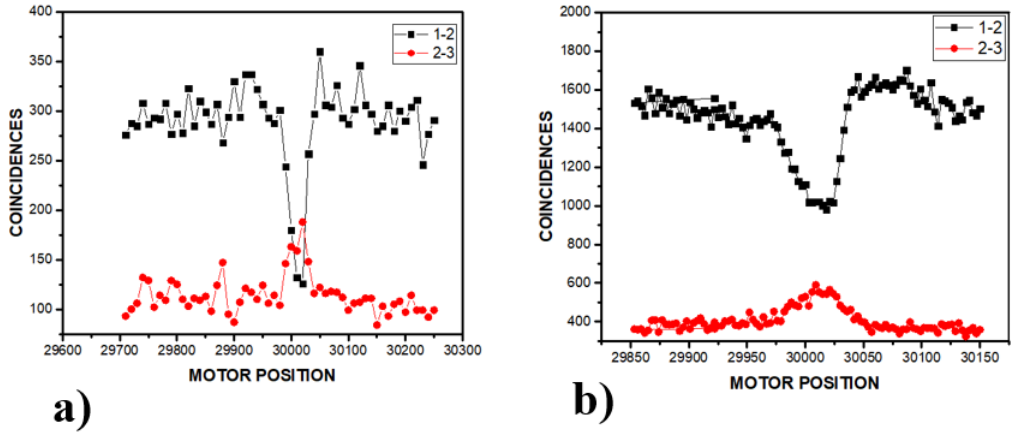

Fig. 4.2: a) Measuring projection onto $|DA\rangle$ (Black) and $|DD\rangle$ (Red) for fourier, b) Measuring projection onto $|DA\rangle$ (Black) and $|DD\rangle$ (Red) for image .

Next we insert a HWP just after the crystal and create a state given in equation (4.61). Again we give a sweep to motor position closed to the interference region and measured projection onto $|DA\rangle$ (Black) and $|DD\rangle$ (Red) as illustrated in figure 4.3. In figure 4.3 measurement **a** corresponds to fourier while the plot **b** corresponds to the image that is obtained by putting lenses after the crystals. We can see from both figures that the plots are thinner for fourier with respect to the image.

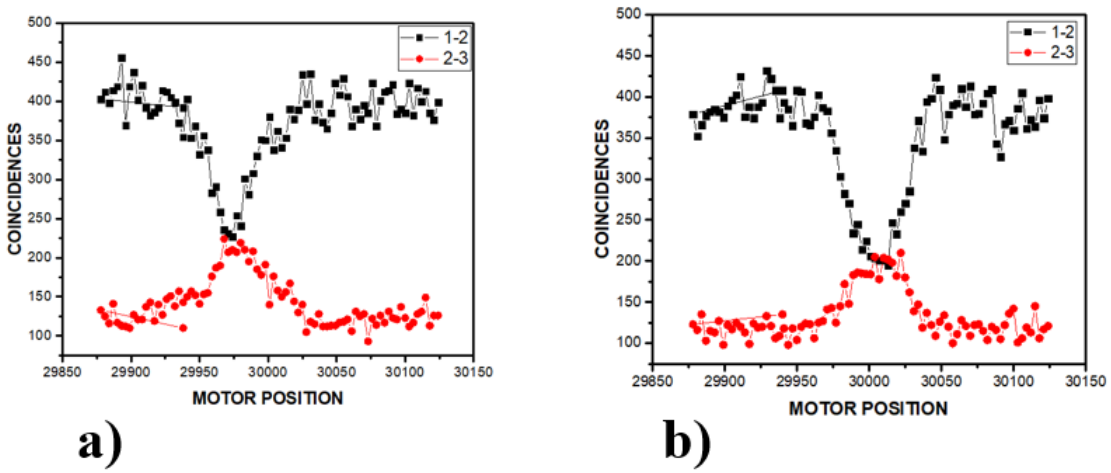

Fig. 4.3: a) Projection plots after HWPc for fourier, b) Image.

Similarly for projecting onto circular basis we put QWP at projection and obtained the plots of coincidences counts verses motor position. Following plots are for the state given in equation (4.47). We give a sweep to motor closed to the region where we have the interference and measured projection onto $|RL\rangle$ as shown in figure 4.4. In figure 4.4 measurement **a** corresponds to fourier for this state while the plot **b** corresponds to the measurment of image of state which is obtained by putting lenses after the crystals.

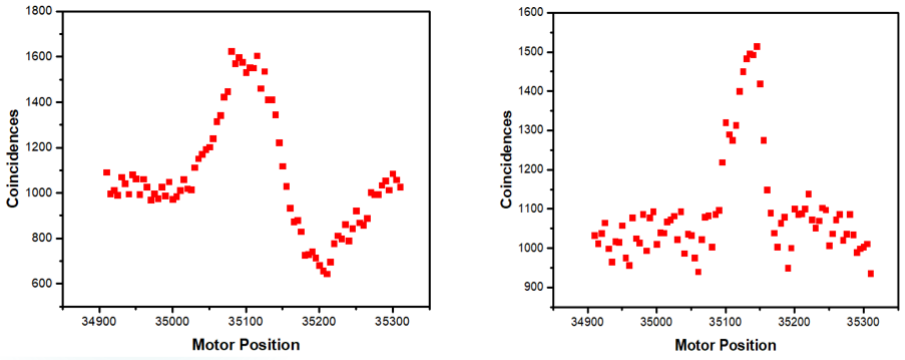

a)Fourier **b)Image**

Fig. 4.4: a) Projection plots for fourier, b) Image.

Next we insert a HWP just after the crystal and create a state given in equation (4.61). Again we give a sweep to motor position closed to the interference region and measured projection onto $|RR\rangle$ as illustrated in figure 4.5. In figure 4.5 measurement **a** corresponds to fourier while the plot **b** corresponds to the image that is obtained by putting lenses after the crystals.

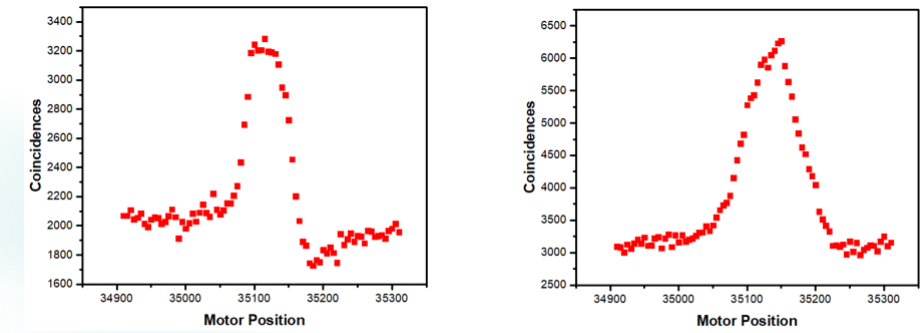

a)Fourier **b)Image**

Fig. 4.5: a) Projection plots after HWPc for Fourier, b) Image.

The coincidences that we obtained for different configurations are shown in the figures 4.2, 4.3, 4.4 and 4.5. We can use these coincidences to obtain the characteristic function for position using the equation (4.25) and (4.26). The equation (4.25) is obtain through coincidences when we measure projection onto diagonal and anti-diagonal ($\theta = 0$), and circular ($\theta = \pi/2$) basis. Similarly, to obtain the expected value of sine in equation (4.26) we also need projection onto $|\frac{\pi}{4}^{\pm}\rangle$ basis ($\theta = \pm\pi/4$). The position and momentum measurement are obtained by change the lens configuration.

Note that the whole characteristic functions can't be obtained because measurements projection $|\frac{\pi}{4}^{\pm}\rangle$ have not been taken. Measurement of whole characteristic functions will be the starting point of my future project.

Chapter 5

Conclusions

In this dissertation we study theoretically and experimentally how the uncertainty relations based on the characteristic function derived in [10] can be used to witness non-Gaussian entanglement of pairs of photons. We developed a technique to obtain the characteristic function a pair of photons performing polarization projection. We calculate the expected characteristic function for our optical setup when the states are pure and mixed. We also experimentally obtained preliminaries results of the probabilities necessary to calculate the characteristic function when the state is Gaussian. Measurements of the characteristic function for non-Gaussian states will be part of future project.

Bibliography

[1] Michael A Nielsen and Isaac Chuang. Quantum computation and quantum information, 2002.

[2] Albert Einstein, Boris Podolsky, and Nathan Rosen. Can quantum-mechanical description of physical reality be considered complete? *Physical review*, 47(10):777, 1935.

[3] John S Bell. On the einstein podolsky rosen paradox. *Physics Physique Fizika*, 1(3):195, 1964.

[4] Alain Aspect, Jean Dalibard, and Gérard Roger. Experimental test of bell's inequalities using time-varying analyzers. *Physical review letters*, 49(25):1804, 1982.

[5] Artur K Ekert. Quantum cryptography based on bell's theorem. *Physical review letters*, 67(6):661, 1991.

[6] Elisabeth Rieper, Janet Anders, and Vlatko Vedral. The relevance of continuous variable entanglement in dna. *arXiv preprint arXiv:1006.4053*, 2010.

[7] Hiroki Takahashi, Jonas S Neergaard-Nielsen, Makoto Takeuchi, Masahiro Takeoka, Kazuhiro Hayasaka, Akira Furusawa, and Masahide Sasaki. Non-gaussian entanglement distillation for continuous variables. *arXiv preprint arXiv:0907.2159*, 2009.

[8] Fabio Dell'Anno, Silvio De Siena, and Fabrizio Illuminati. Realistic continuous-variable quantum teleportation with non-gaussian resources. *Physical Review A*, 81(1):012333, 2010.

[9] Samuel L Braunstein and Peter Van Loock. Quantum information with continuous variables. *Reviews of Modern Physics*, 77(2):513, 2005.

[10] Łukasz Rudnicki, Daniel S Tasca, and Stephen P Walborn. Uncertainty relations for characteristic functions. *Physical Review A*, 93(2):022109, 2016.

[11] DN Klyshko, AN Penin, and BF Polkovnikov. Parametric luminescence and light scattering by polaritons. *Soviet Journal of Experimental and Theoretical Physics Letters*, 11:5, 1970.

[12] David C Burnham and Donald L Weinberg. Observation of simultaneity in parametric production of optical photon pairs. *Physical Review Letters*, 25(2):84, 1970.

[13] Daniel M Greenberger, Michael Horne, and Anton Zeilinger. Bell theorem without inequalities for two particles. i. efficient detectors. *Physical Review A*, 78(2):022110, 2008.

[14] R. Ghosh and L. Mandel. Observation of nonclassical effects in the interference of two photons. *Phys. Rev. Lett.*, 59:1903–1905, Oct 1987.

[15] Jeremy L O'brien. Optical quantum computing. *Science*, 318(5856):1567–1570, 2007.

[16] JY Cheung, CJ Chunnilall, ER Woolliams, NP Fox, JR Mountford, J Wang, and PJ Thomas. The quantum candela: a re-definition of the standard units for optical radiation. *Journal of Modern Optics*, 54(2-3):373–396, 2007.

[17] Nicolas Gisin, Grégoire Ribordy, Wolfgang Tittel, and Hugo Zbinden. Quantum cryptography. *Reviews of modern physics*, 74(1):145, 2002.

[18] Christophe Couteau. Spontaneous parametric down-conversion. *Contemporary Physics*, 59(3):291–304, 2018.

[19] Anthony Martin, Amandine Issautier, Harrald Herrmann, Wolfgang Sohler, Daniel Barry Ostrowsky, Olivier Alibart, and Sébastien Tanzilli. A polarization entangled photon-pair source based on a type-ii ppln waveguide emitting at a telecom wavelength. *New Journal of Physics*, 12(10):103005, 2010.

[20] Paul G Kwiat, Klaus Mattle, Harald Weinfurter, Anton Zeilinger, Alexander V Sergienko, and Yanhua Shih. New high-intensity source of polarization-entangled photon pairs. *Physical Review Letters*, 75(24):4337, 1995.

[21] Paul G Kwiat. E, waks, ag white, i. appelbaum, and ph eberhard. *Phys. Rev. A*, 60:R867, 1999.

[22] Paul R Tapster, John G Rarity, and PCM Owens. Violation of bell's inequality over 4 km of optical fiber. *Physical Review Letters*, 73(14):1923, 1994.

[23] JG Rarity and PR Tapster. Experimental violation of bell's inequality based on phase and momentum. *Physical Review Letters*, 64(21):2495, 1990.

[24] RS Thebaldi. *Estados de Dois Fótons com Momento Angular Orbital*. PhD thesis, Dissertation Thesis. Supervised by Carlos Henrique Monken. Minas Gerais, UFMG, 2001.

[25] Alois Mair, Alipasha Vaziri, Gregor Weihs, and Anton Zeilinger. Entanglement of the orbital angular momentum states of photons. *Nature*, 412(6844):313, 2001.

[26] Stephen P Walborn, CH Monken, S Pádua, and PH Souto Ribeiro. Spatial correlations in parametric down-conversion. *Physics Reports*, 495(4-5):87–139, 2010.

[27] Milena D'Angelo, Yoon-Ho Kim, Sergei P Kulik, and Yanhua Shih. Identifying entanglement using quantum ghost interference and imaging. *Physical review letters*, 92(23):233601, 2004.

[28] John C Howell, Ryan S Bennink, Sean J Bentley, and RW Boyd. Realization of the einstein-podolsky-rosen paradox using momentum-and position-entangled photons from spontaneous parametric down conversion. *Physical Review Letters*, 92(21):210403, 2004.

[29] Stefano Mancini, Vittorio Giovannetti, David Vitali, and Paolo Tombesi. Entangling macroscopic oscillators exploiting radiation pressure. *Physical review letters*, 88(12):120401, 2002.

[30] Lu-Ming Duan, Géza Giedke, Juan Ignacio Cirac, and Peter Zoller. Inseparability criterion for continuous variable systems. *Physical Review Letters*, 84(12):2722, 2000.

[31] Rajiah Simon. Peres-horodecki separability criterion for continuous variable systems. *Physical Review Letters*, 84(12):2726, 2000.

[32] Gerardo Adesso and Fabrizio Illuminati. Entanglement in continuous-variable systems: recent advances and current perspectives. *Journal of Physics A: Mathematical and Theoretical*, 40(28):7821, 2007.

[33] Evegny Shchukin and Werner Vogel. Inseparability criteria for continuous bipartite quantum states. *Physical review letters*, 95(23):230502, 2005.

[34] Samuel L Braunstein, Ady Mann, and Michael Revzen. Maximal violation of bell inequalities for mixed states. *Physical Review Letters*, 68(22):3259, 1992.

[35] Lev Vaidman. Teleportation of quantum states. *Physical Review A*, 49(2):1473, 1994.

[36] Charles H Bennett and Gilles Brassard. Quantum cryptography: public key distribution and coin tossing. *Theor. Comput. Sci.*, 560(12):7–11, 2014.

[37] Charles H Bennett and Stephen J Wiesner. Communication via one-and two-particle operators on einstein-podolsky-rosen states. *Physical review letters*, 69(20):2881, 1992.

[38] Artur Ekert and Richard Jozsa. Shor's quantum algorithm for factorising numbers. *Rev. Mod. Phys*, 68:733–753, 1996.

[39] Asher Peres. Separability criterion for density matrices. *Physical Review Letters*, 77(8):1413, 1996.

[40] Mark Hillery and M Suhail Zubairy. Entanglement conditions for two-mode states. *Physical review letters*, 96(5):050503, 2006.

[41] Hyunchul Nha and M Suhail Zubairy. Uncertainty inequalities as entanglement criteria for negative partial-transpose states. *Physical review letters*, 101(13):130402, 2008.

[42] Girish Saran Agarwal and Asoka Biswas. Inseparability inequalities for higher order moments for bipartite systems. *New Journal of Physics*, 7(1):211, 2005.

[43] Hyunchul Nha and Jaewan Kim. Entanglement criteria via the uncertainty relations in su (2) and su (1, 1) algebras: Detection of non-gaussian entangled states. *Physical Review A*, 74(1):012317, 2006.

[44] E Shchukin and W Vogel. Universal measurement of quantum correlations of radiation. *Physical review letters*, 96(20):200403, 2006.

[45] SP Walborn, AH Pimentel, L Davidovich, and RL de Matos Filho. Quantum-enhanced sensing from hyperentanglement. *Physical Review A*, 97(1):010301, 2018.